HITACHI

GE Hitachi Nuclear Energy

Richard E. Kingston
Vice President, ESBWR Licensing

P.O. Box 780
3901 Castle Hayne Road, M/C A-65
Wilmington, NC 28402 USA

T 910.819.6192
F 910.362.6192
rick.kingston@ge.com

MFN 09-571

Docket No. 52-010

August 27, 2009

U.S. Nuclear Regulatory Commission
Document Control Desk
Washington, D.C. 20555-0001

Subject: **Response to NRC RAI Letter No. 363 Related to ESBWR Design Certification Application – DCD Tier 2 Section 3.8 – Seismic Category I Structures; RAI Number 3.8-94 S05**

The purpose of this letter is to submit the GE Hitachi Nuclear Energy (GEH) response to U.S. Nuclear Regulatory Commission (NRC) Request for Additional Information (RAI) letter number 363 sent by NRC letter dated August 3, 2009 (Reference 1). RAI Number 3.8-94 S05 is addressed in Enclosure 1.

If you have any questions or require additional information, please contact me.

Sincerely,

Richard E. Kingston

Richard E. Kingston
Vice President, ESBWR Licensing

Reference:

1. MFN 09-541 Letter from U.S. Nuclear Regulatory Commission to J. G. Head, GEH, *Request For Additional Information Letter No. 363 Related to ESBWR Design Certification* dated August 3, 2009

Enclosure:

1. Response to NRC RAI Letter No. 363 Related to ESBWR Design Certification Application - DCD Tier 2 Section 3.8 – Seismic Category I Structures; RAI Number 3.8-94 S05

cc:	AE Cubbage	USNRC (with enclosures)
	JG Head	GEH/Wilmington (with enclosures)
	DH Hinds	GEH/Wilmington (with enclosures)
	eDRF Section	0000-0106-2243 (RAI 3.8-94 S05)

ENCLOSURE 1

MFN 09-571

Response to NRC RAI Letter No. 363
Related to ESBWR Design Certification Application[1]

DCD Tier 2 Section 3.8 – Seismic Category I Structures

RAI Number 3.8-94 S05

[1] Original Response, Supplement 1, Supplement 2, Supplement 3 and Supplement 4 previously submitted under MFNs 06-407; 06-407, Supplement 2; 06-407, Supplement 3; 06-407, Supplement 13 and 09-388 without DCD updates are included to provide historical continuity during review.

NRC RAI 3.8-94

DCD Section 3.8.5.4 indicates that the design incorporates an evaluation of the worst loads resulting from the superstructures and loads directly applied to the foundation mat, due to static and dynamic load combinations. However, the DCD does not identify the maximum allowable toe pressure that is acceptable for the basemat design, under the worst-case static and dynamic loads. This information is needed so that evaluations can be made at the COL state for site-specific conditions. Include the maximum toe pressure used in the basemat design in DCD Table 3.8-13.

GE Response

Maximum soil bearing stresses involving SSE are summarized in DCD Tier 2 Table 3G.1-58 for soft, medium and hard site conditions. Maximum soil bearing stress due to dead plus live loads is 699 kPa as shown in DCD Tier 2 Appendix 3G.1.5.5. The site-specific allowable bearing capacities need to be larger than the maximum stress depending on its site condition.

The values indicated in DCD Tier 2 Table 3G.1-58 are evaluated by using the Energy Balance Method, which is described in the Reference cited in response to NRC RAI 3.7-48, Supplement 1. In the evaluations, the basemat is assumed to be rigid, and uplift of the basemat is considered.

The soil pressures obtained from the RB/FB global FE model analyses used for the basemat section design are summarized in Table 3.8-94(1). This table also includes the results of the basemat uplift analyses, which were performed to respond NRC RAI 3.8-13. Seismic loads used for the FE analyses are worst-case loads, i.e., the enveloped values for all site conditions included in DCD Tier 2 Table 3G.1-58. In the FE analyses, the basemat is assumed to be flexible.

As shown in Table 3.8-94(1), the bearing pressures obtained by the FE analyses are less than the worst case maximum bearing pressure in DCD Tier 2 Table 3G.1-58, which is 5.33 MPa for the hard site. Therefore, it can be concluded that the maximum bearing pressures in DCD Tier 2 Table 3G.1-58 are evaluated conservatively.

Table 3.8-94(1) Maximum Bearing Pressure

Seismic Direction	Case	Max. Pressure (MPa)	Location	Combination
NS	DCD	4.18	Northeast	1.0NS+0.4EW+0.4V
	Uplift *1	4.56	Northeast	1.0NS+0.4EW+0.4V
EW	DCD	4.16	Northeast	0.4NS+1.0EW+0.4V
	Uplift *1	4.49	Northeast	0.4NS+1.0EW+0.4V

Note *1: See response to NRC RAI 3.8-13, Supplement 1.

NRC RAI 3.8-94, Supplement 1

NRC Assessment Following the December 14, 2006 Audit

GE's response refers to Table 3G.1-58 which provides the maximum soil bearing stress involving SSE. GE needs to clarify that the values in Table 3G.1-58 represent the maximum soil bearing stress for all load combinations. GE also needs to explain whether the comparisons to the bearing pressures in Table 3.8-94(1) are for the same load combinations.

During the audit, GE provided a draft supplemental response to address the above. Regarding the first question, GE provided an acceptable response. GE needs to clarify the RAI response and the draft supplemental response regarding the comparison of the maximum bearing pressures reported in Table 3.8-94(1) to Table 3.G.1-58. GE also needs to explain why the toe pressures reported in Table 3G.1-58 are conservative when considering the variation of horizontal soil springs as discussed in RAI 3.8-93.

GE Response

The values in DCD Tier 2 Table 3G.1-58 represent the maximum soil bearing stress for all combinations calculated using the Energy Balance Method for the RB/FB (Reference 1). They are the maximum bearing stresses for the three generic soil conditions. The toe pressures presented in Table 3.8-94(1) are calculated using the global FE model for design seismic forces which envelope the responses of three soil conditions. The methods of analysis are different in the two calculations. Table 3.8-94(2) compares the maximum soil bearing pressures calculated by the Energy Balance Method and the linear FEM analysis. The results show that the Energy Balance Method is a more conservative method to use for the determination of soil bearing pressures. Note that the values obtained by the Energy Balance Method shown in Table 3.8-94(2) are the updated values for DCD Tier 2 Table 3G.1-58, due to the changes in seismic design loads, which have been included in DCD Tier 2 Revision 3.

Reference 1: Tseng, W.S. and Liou, D.D., "Simplified Methods for Predicting Seismic Basemat Uplift of Nuclear Power Plant Structures, Transactions of the 6th International Conference on SmiRT", Paris, France, August 1981

Table 3.8-94(2) Comparison of Maximum Bearing Pressure

		Site Condition (MPa)		
		Soft	Medium	Hard
Energy Balance Method		2.7	7.3	5.4
FEM	Linear	2.6	4.8	5.4
	Uplift*	-	-	5.4

* See response to NRC RAI 3.8-13, Supplement 1. The tension springs of linear cases are eliminated.

The variations of horizontal soil spring ("Hard Spot" and "Soft Spot" as shown in the response to NRC RAI 3.8-93, Supplement 1) are also considered in this study. Note that the DCD envelope is based on uniform soil conditions. Despite the fundamental difference in the treatment of the soil stiffness distribution, the maximum soil bearing pressures of the non-uniform soil condition are similar to those of the uniform soil condition.

Table 3.8-94(3) Maximum Bearing Pressure Under Non-Uniform Soil Condition

	Case	Max. Pressure (MPa)
FEM	Hard Spot*	3.8
	Soft Spot*	4.9

* See response to NRC RAI 3.8-93, Supplement 1. Stiffer area is Softx3 condition.

DCD Tier 2 Subsections 3G.1.5.5, 3G.1.6, Table 3G.1-58 and Table 3G.2-27 have been revised. The pages (pp. 3G-16, 3G-18, 3G-123 & 3G-215) revised in DCD Tier 2 Revision 3 for this response are attached.

DCD Impact

No DCD change was made in response to this RAI Supplement.

NRC RAI 3.8-94, Supplement 2

NRC Assessment from Chandu Patel E-mail Dated May 24, 2007

The staff requests the applicant to address the following:

(1) The bearing stresses reported in DCD Tier 2 Table 3G.1-58 for soft, medium and hard site conditions are 2.7 MPa (56.4 ksf), 7.3 Mpa (152.6 ksf) and 5.4 MPa (112.9 ksf). These values are extremely large compared to known soil and rock capacities. Explain how the COL applicant will satisfy this criteria. Also explain why the bearing stress reported for the medium site condition (7.3 MPa) is higher than the hard site condition (5.4 MPa).

(2) Explain how the COL applicant is to use the maximum bearing pressures reported in DCD Tier 2 Table 3G.1 58 and Table 3G.2 27 when conditions for a specific site fall between the tabulated values for soft, medium and hard site conditions.

(3) Footnote 7 to DCD Tier 2 Table 2.0-1 references DCD Tier 2 Subsections 3G.1.5.5, 3G2.5.5 and 3G.3.5.5 for the minimum dynamic bearing capacities for the Reactor, Control and Fuel Building, respectively. However, Footnote 7 to the corresponding DCD Tier 1 Table 5.1-1 only states "At foundation level of Seismic Category I structures." Explain why the minimum dynamic bearing capacities are not clearly specified as Tier 1 information.

(4) The response to RAI 3.8-94 states that variations in the horizontal soil spring were considered and concludes that the maximum soil bearing pressures of the nonuniform soil condition are similar to those of the uniform soil condition. Results for maximum bearing pressure under non-uniform soil conditions are presented in Table 3.8-94(3). To complete the response, for the nonuniform soil conditions considered in Table 3.8-94(3), provide comparisons of the bending moments across the basemat in both directions that demonstrate that the DCD design moments bound the moments for the nonuniform soil condition.

GEH Response

(1) Confirmation of bearing capacity is a COL item as stated in DCD Tier 2 Table 2.0-1. The higher bearing stress at the medium site condition is due to the higher spectral acceleration of the input ground motion response spectra at the SSI fundamental frequencies as shown in Figure 3.8-94(1) in comparison with other site conditions for each direction. Consequently, the envelope of the soil reaction forces, which are the basis for calculating the bearing pressures, are the largest at the medium site as shown in Table 3.8-94(4).

(2) When specific site conditions fall between the cases specified, the larger value within the applicable range applies. Alternatively, a linearly interpolated value

may be used and is clarified in footnotes to DCD Tier 2 Revision 4 Tables 3G.1-58 and 3G.2-27. The revised pages 3G-123 and 3G-228 in DCD Tier 2 Revision 4 are attached.

(3) Minimum dynamic bearing capacities have been included in DCD Tier 1 Revision 4 Table 5.1-1. The revised page 5.1-3 in DCD Tier 1 Revision 4 is attached.

(4) Table 3.8-94(3) is a summary of the analyses results presented in the response to NRC RAI 3.8-93, Supplement 1. The comparisons of the bending moments across the basemat were provided in Figure 3.8-93(16)-c. In that figure Hard Spot case is higher than DCD condition. The allowable bending moment at the top surface of the basemat is 16.7 MNm/m using the rebar ratio (0.321%) shown in DCD Tier 2 Table 3G.1-50. Therefore, it is concluded that the hard spot results do not affect section design in the DCD. Also, DCD Tier 2 Tables 3G.1-51 through 3G.1-55 show rebar and concrete stresses. These calculated stresses are sufficiently lower than Code allowable limits.

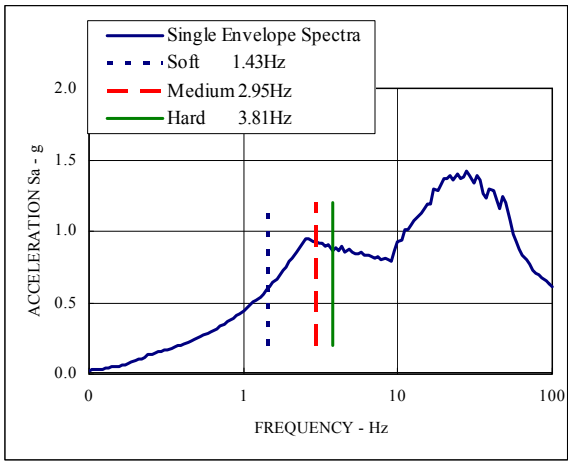

(a) NS Direction

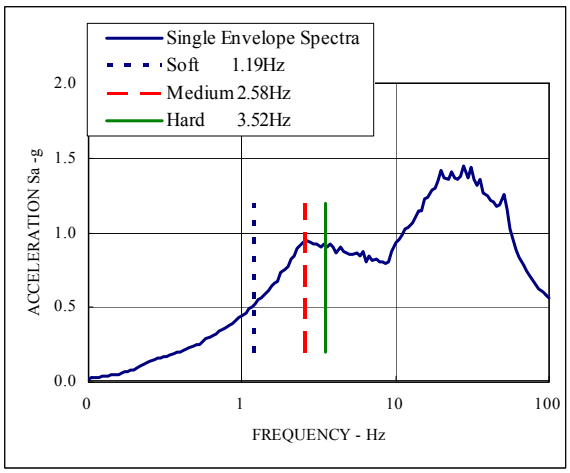

(b) EW Direction

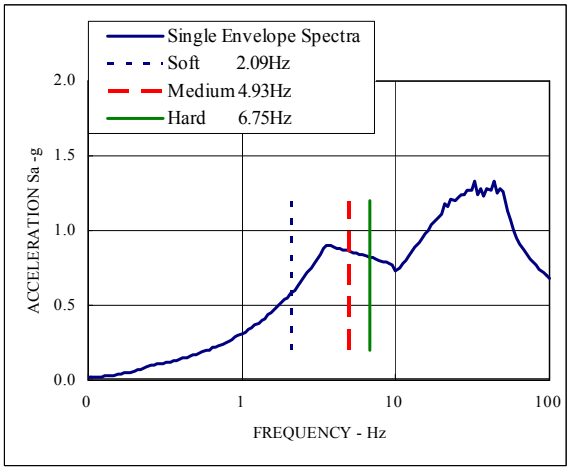

(c) Vertical Direction

Figure 3.8-94(1) Input Motion Spectra and RBFB SSI Fundamental Frequencies

Table 3.8-94(4) Soil Spring Reaction for RBFB Seismic Model

	Envelope Soil Reaction	
Soft	N(MN)	M(MNm)
NS	-	22094
EW	-	31999
V	676	-
Bearing Pressure	2.7 Mpa	
Medium	N(MN)	M(MNm)
NS	-	48131
EW	-	58908
V	1148	-
Bearing Pressure	7.3 Mpa	
Hard	N(MN)	M(MNm)
NS	-	50238
EW	-	47061
V	1003	-
Bearing Pressure	5.4 Mpa	

DCD Impact

No DCD change was made in response to this RAI Supplement.

NRC RAI 3.8-94, Supplement 3

The RAI Supplement 2 response, transmitted in GEH letter dated November 28, 2007, provided information to address five items related to the soil bearing capacities. GEH is requested to addresses the following items:

(1) The staff agrees with the statement made in the GEH response that confirmation of the bearing capacity is a COL item. However, the development of the required bearing capacities is part of the DCD review and if the values are extremely large compared to known soil and rock capacities, the staff needs to have a reasonable assurance that these bearing capacities can be met. Therefore, GEH is requested to explain why these extremely large bearing capacities are considered to be reasonable values which can be met at various potential plant sites.

(2) GEH is requested to explain why it is acceptable to use a linearly interpolated value for the soil bearing capacities between the three sets of values (soft, medium, and hard). Using the information presented in Figure 3.8-94(1) (c) of the response (as an example), this would underpredict the required bearing capacity.

(3) Footnotes are still missing in the revised Table 5.1-1 in DCD Tier 1 Revision 4.

Revised GEH Response

(1) The large RB/FB and CB minimum dynamic soil bearing capacities in DCD Revision 5 are considered to be conservative and have been reduced in DCD Revision 6 based on the below recalculation.

The minimum dynamic soil bearing capacities in DCD Revision 5 were determined from bearing pressure demand calculations for foundation stability analyses. These analyses contained conservatisms as follows:

a) Although the RB/FB and the CB are deeply embedded structures, the seismic soil reactions calculated by the DAC3N soil-spring SSI analyses without the embedment effect were used for the stability analysis for these buildings. This extra conservatism is removed in the below bearing pressure demand recalculation in which the seismic soil reactions obtained from the SASSI2000 analyses, which take into account embedment, are used.

b) The bearing forces were calculated by the Energy Balance Method for three cases NS+UD, EW+UD, and UD (vertical). The maximum toe pressures from these cases were then combined by the 100/40/40 method. In this approach the dead weight of the building and vertical seismic load were included in vertical “UD” in all three cases resulting in triple counting of the vertical load effect.

Therefore, the minimum dynamic soil bearing capacities (maximum dynamic soil bearing stress involving SSE plus static) are recalculated as follows:

1. Calculation of Overturning Moment from the SASSI2000 Results

Vertical soil reaction force time histories from the separate NS, EW and UD (vertical) SASSI2000 analyses at each node of the SASSI2000 basemat model are first added by the algebraic sum method since the input motions of the three components are mutually statistically independent. The overall vertical force time history for the basemat is calculated by summing up the reaction forces at all nodes. The overturning moment time histories for both directions are then calculated from the nodal vertical time histories by using the following equations:

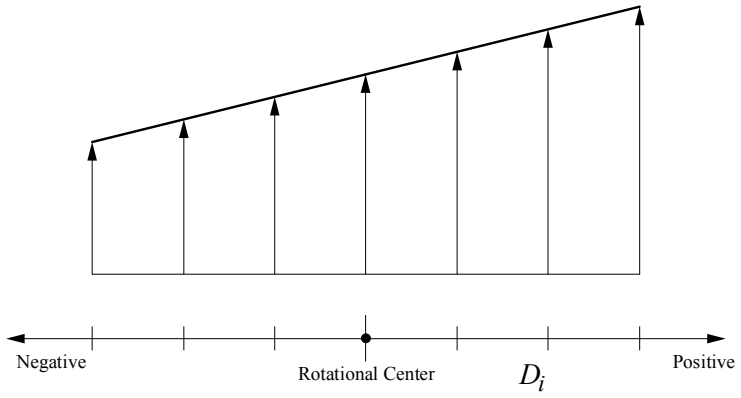

$$_{time=T}M = \sum D_i \cdot {}_{time=T}V_i$$

$$_{time=T}V_i = {}_{time=T}V_{NS} + {}_{time=T}V_{EW} + {}_{time=T}V_{UD}$$

$_{time=T}V_{NS}$: Vertical seismic force at T sec due to NS (X-dir) excitation

$_{time=T}V_{EW}$: Vertical seismic force at T sec due to EW(Y-dir) excitation

$_{time=T}V_{UD}$: Vertical seismic force at T sec due to UD (Z-dir) excitation

The bearing pressures are evaluated at the possible three timings when the NS (M_x) moment, the EW (M_y) moment or the vertical force (V) each becomes maximum, i.e.:

M_{x_max},	M_y @ time T of M_{x_max},	V @ time T of M_{x_max}
M_{y_max},	M_x @ time T of M_{y_max},	V @ time T of M_{y_max}
Vmax,	Mx @ time T of Vmax,	My @ time T of Vmax

And then the three bearing pressures are enveloped.

2. Evaluation Method of Bearing Pressure from Three Forces, ${}_TM_x$, ${}_TM_y$, ${}_TN$

As for the vertical loads, ${}_TN$, the following two cases are considered:

Max. ${}_TN = W + {}_TV$

Min. ${}_TN = W - B - {}_TV$

where, “W” is the building weight and “B” is the buoyancy force

If $M_x/Z_x > M_y/Z_y$, the following procedure is used (if $M_x/Z_x < M_y/Z_y$, switch M_y for M_x):

a) Calculate bearing pressure, ${}_TBP_x$, per the Energy Balance Method using ${}_TM_x$ and ${}_TN$

b) Calculate bearing pressure, ${}_TBP_y$, per the following equation using ${}_TM_y$:

${}_TBP_y = {}_TM_y / Z_y$

$Z_y = CL \cdot CW^2 / 6$ (considering the contact area)

c) Calculate total bearing pressure ${}_TBP$:

${}_TBP = {}_TBP_x + {}_TBP_y$

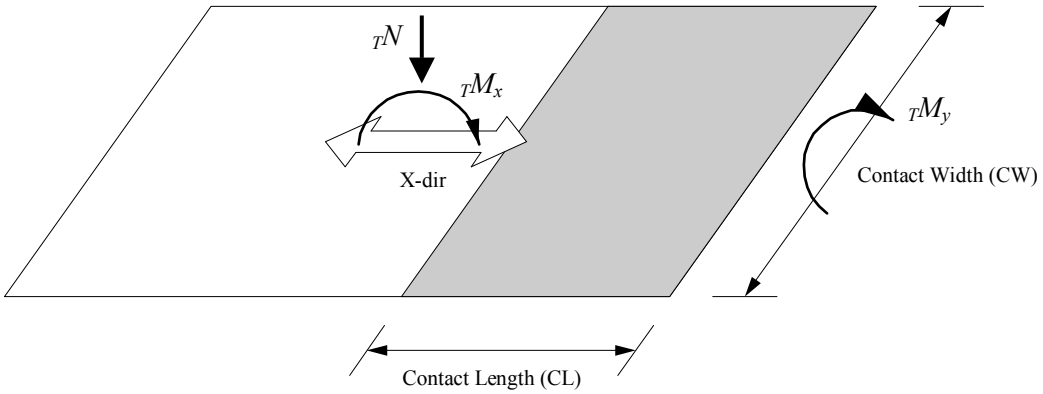

3. Evaluation Results

Bearing pressures are evaluated by the above method using the SASSI2000 results for three uniform sites (RU-8 with embedment for RB/FB, CU-4 with embedment for CB and FU-2 without embedment for surface founded FWSC) and the layered sites considered in the DCD. DCD Tier 2 Subsections 3.7.1.1.3, 3A.5, 3A.5.2, 3A.6, 3C.7.1.3, 3C.7.2.1 and 3C.7.2.3 and Tables 3.7-3 and 3A.6-1 will be updated in Revision 6 accordingly.

The layered site cases L-2 and L-4 are excluded for the RB/FB and CB in the stability evaluation. The calculated basemat interface loads with the supporting soil for these two sites are large as compared to those for other generic site conditions analyzed. This may be attributed to the large contrast in shear wave velocities in adjacent soil layers assumed for these two layered sites for which the shear wave velocity ratio of the soil layer below the foundation to the soil layer above the foundation is larger than 2.5.

To be consistent with this limitation, a new site interface parameter for maximum ratio of soil shear wave velocity in adjacent layers will be added in DCD Tier 2 Table 2.0-1 in Revision 6 to ensure that the site soil layering does not have as large a contrast in shear wave velocities as the generic layered sites L-2 and L-4 (see DCD Tier 2 Table 3A.3-3 for description of layered sites) as follows:

Bottom 20 m (66 ft) layer to top 20 m (66 ft) layer: 2.5 ratio

Bottom 40 m (131 ft) layer to top 20 m (66 ft) layer: 2.5 ratio

Adjacent layers are the two layers with a total depth of 40 m (131 ft) or 60 m (197 ft) below grade. The first layer, termed top layer, covers the top 20 m (66 ft). The second layer, termed bottom layer, covers the next 20 m (66 ft) or 40 m (131 ft). The ratio is the average velocity of the bottom layer divided by the average velocity of the top layer. Either the lower bound seismic strain (i.e., strain compatible) profile or the best estimate low strain profile can be used because only the velocity ratio is of interest. This velocity ratio condition does not apply to the FWSC nor to the RB/FB and CB if founded on rock-like material having a shear wave velocity of 1067 m/sec (3500 ft/sec) or higher.

The minimum dynamic soil bearing capacities (maximum dynamic soil bearing stress involving SSE plus static) obtained are shown in Table 3.8-94(5). DCD Tier 1 Table 5.1-1, DCD Tier 2 Tables 2.0-1, 3G.1-58, 3G.2-27 and 3G.4-23 will be revised in Revision 6 with these updated capacities.

The SASSI2000 results of uniform sites (RU-8 for RB/FB, CU-4 for CB and FU-2 for FWSC) are compared with the DAC3N results (RU-3 for RB/FB, CU-3 for CB and FU-1 for FWSC) for floor response spectra as discussed below.

Comparisons of the response spectra are shown in Figures 3.8-94(4) through 3.8-94(15), Figures 3.8-94(16) through 3.8-94(27), and Figures 3.8-94(28) through 3.8-94(39), respectively for the X direction, Y direction, and Z direction. These comparisons will be added in DCD Revision 6 as DCD Tier 2 Figures 3A.8.7-1a through 3A.8.7-3l.

As for the RB/FB, it is found from the results that the responses for the SASSI2000 uniform cases are bounded by the broadened envelope responses of the DAC3N cases in the whole frequency range. The responses of the RU-8 uniform hard site at the vent wall top (X direction per Figure 3.8-94(6)) and the refueling floor (Z direction per (Figure 3.8-94(28)) at around 20 Hz are slightly higher around 20 Hz but the exceedance is negligibly small.

On the other hand, the response spectra of a portion of the CB above ground and the FPE in the FWSC exceeded greater than 10% at the broadened envelope responses of the DAC3N cases in the higher frequency range.

Thus, the SASSI2000 uniform site results of the CB and the FWSC are included where appropriate to obtain the enveloping design spectra. DCD Tier 2 Figures 3A.9-1g, 3A.9-1l, 3A.9-2g and 3A.9-3g will be revised in Revision 6 accordingly.

The uniform site SASSI2000 results for seismic forces of building structural members are less than the DAC3N results, thus there is no impact on the design envelope loads.

DCD Tier 2 Subsection 3A.8.7 and Table 3A.8.7-1 will be updated and DCD Tier 2 Subsection 3A.9.3 will be added in Revision 6 to incorporate the above discussion.

(2) The linear interpolation method is adequate to evaluate maximum dynamic soil bearing pressures for sites within the applicable range of shear wave velocities considered in the DCD.

In accordance with NRC RAI 3.8-94, Supplement 2, Figure 3.8-94(1) (c), the vertical input response spectrum peaks at 3.57 Hz in the frequency range between 2.09 Hz for the soft site and 4.93 Hz for the medium site. This peak vertical frequency is 73% of the vertical SSI fundamental frequency at the medium site.

Applying the same frequency ratio to the horizontal SSI frequencies of the medium site, the horizontal SSI fundamental frequencies for the 3.57 Hz vertical frequency site (termed “intermediate site” hereafter) are found to be 2.14 Hz and 1.87 Hz in the NS and EW directions, respectively. The corresponding spectral accelerations are 0.85g, 0.76g and 0.9g in the NS, EW and vertical directions, respectively, and the corresponding ratios to the medium site spectral accelerations are 0.91, 0.8 and 1.05, as shown in Figure 3.8-94(2).

These spectral acceleration ratios are then applied to the SSE base moment and SSE vertical load of the medium site to obtain the corresponding loads for the intermediate site in the bearing pressure calculation and the maximum bearing pressure for the intermediate site is found to be 1.39 MPa.

This calculated value agrees with the value obtained by the linear interpolation of bearing pressures between the soft and medium sites as illustrated in Figure 3.8-94(3), in which the shear wave velocity value of 561 m/sec for the intermediate site (3.57 Hz) is linearly interpolated from 300 m/sec soft site (2.09 Hz) and 800 m/sec medium site (4.93 Hz).

(3) DCD Tier 1 Table 5.1-1 has been revised in Revision 5 to retain only those footnotes in DCD Tier 2 Table 2.0-1 that are intrinsic to the description of the ESBWR Standard Plant site design parameter and are not background information for the parameter. Please see the GEH response to NRC RAI 2.0-1 transmitted to the NRC on March 24, 2008 via MFN 08-248.

Table 3.8-94(5) Maximum Dynamic Soil Bearing Stress Involving SSE + Static (MPa)

Building	Site Condition		
	Soft (V_s = 300 m/sec)	Medium (V_s = 800 m/sec)	Hard ($V_s \geq$ 1700 m/sec)
RB/FB	1.2	1.5	1.1
CB	0.44	2.2	0.42
FWSC	0.46	0.69	1.2

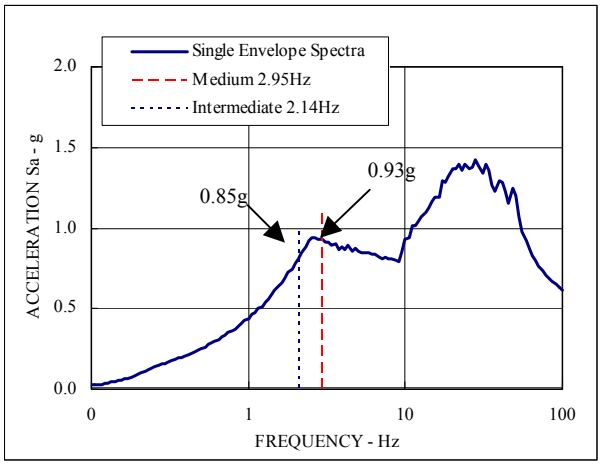

(a) NS Direction

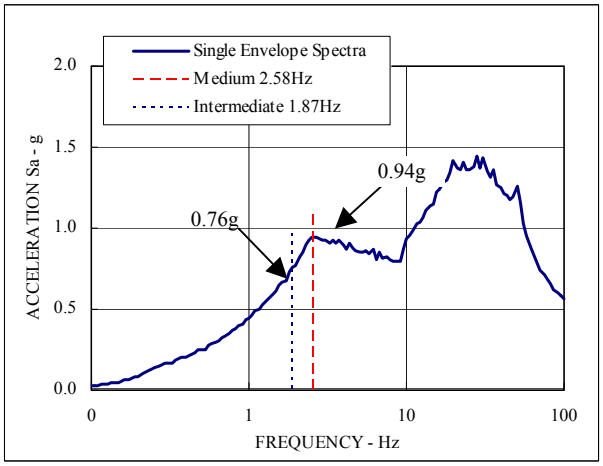

(b) EW Direction

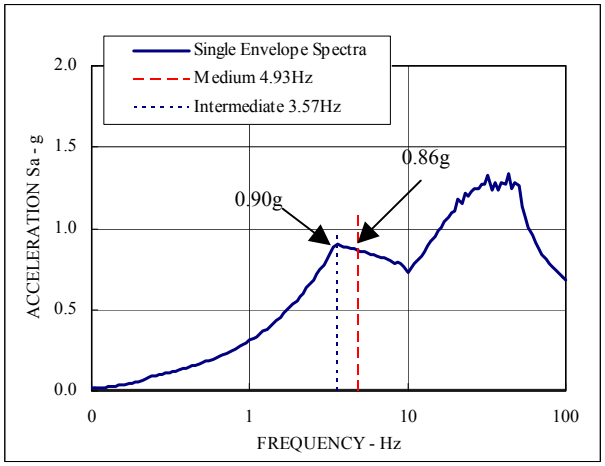

(c) Vertical Direction

Figure 3.8-94(2) Input Motion to Intermediate Site

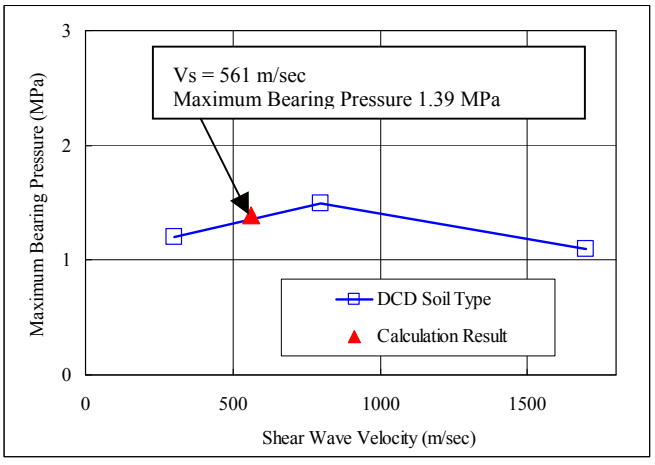

V_s Interpolation:

Medium Site: f = 4.93 Hz, V_s = 800 m/sec
Soft Site: f = 2.09 Hz, V_s = 300 m/sec

Hence,

Intermediate Site: f = 3.57 Hz, V_s = 561 m/sec

Figure 3.8-94(3) Calculated vs. Interpolated Bearing Pressures

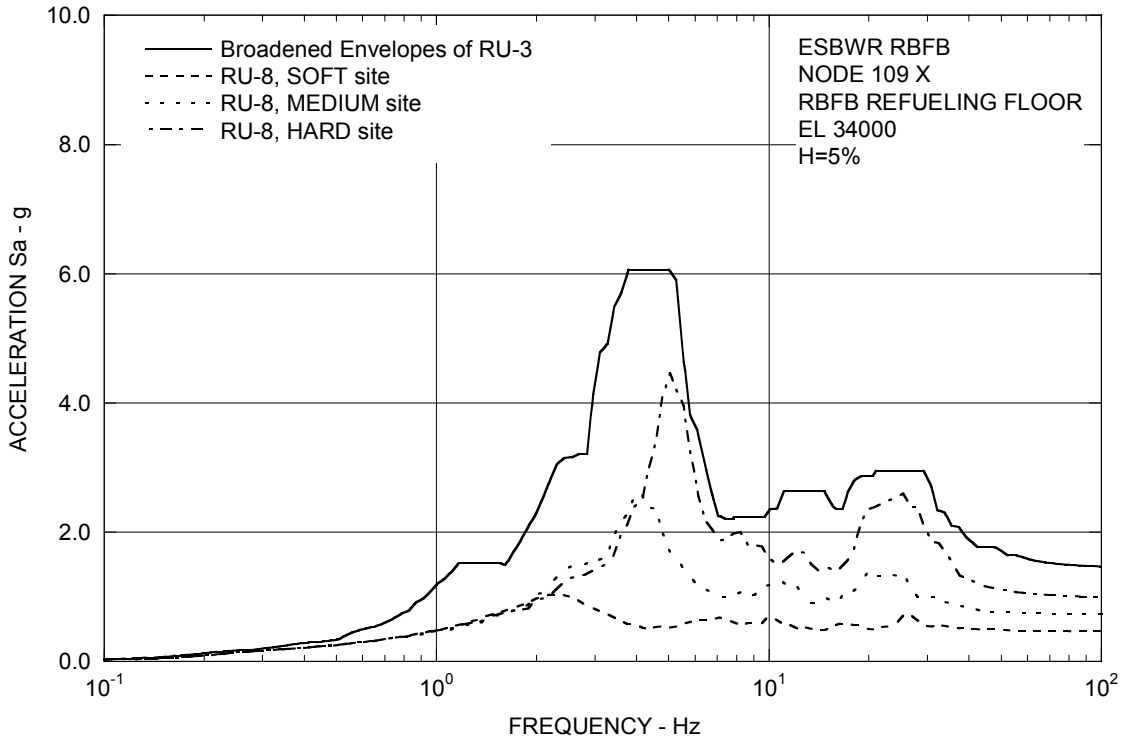

Figure 3.8-94(4) FRS (Compared with the DAC3N) – RBFB Refueling Floor X

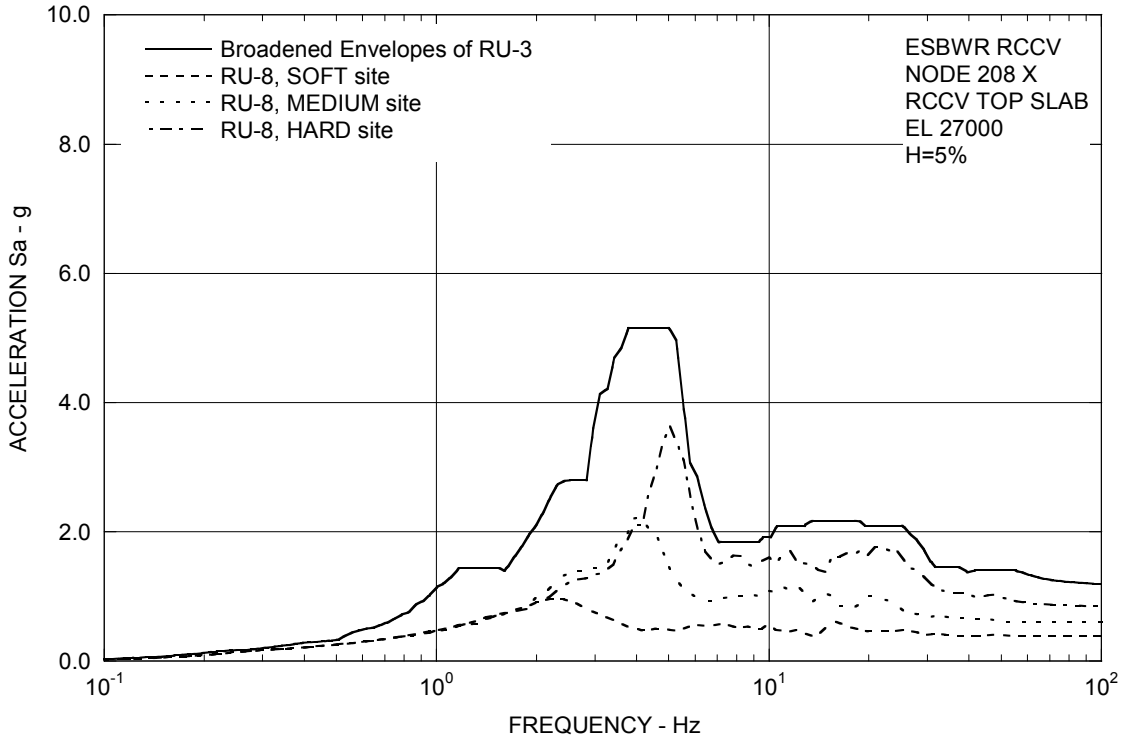

Figure 3.8-94(5) FRS (Compared with the DAC3N) – RCCV Top Slab X

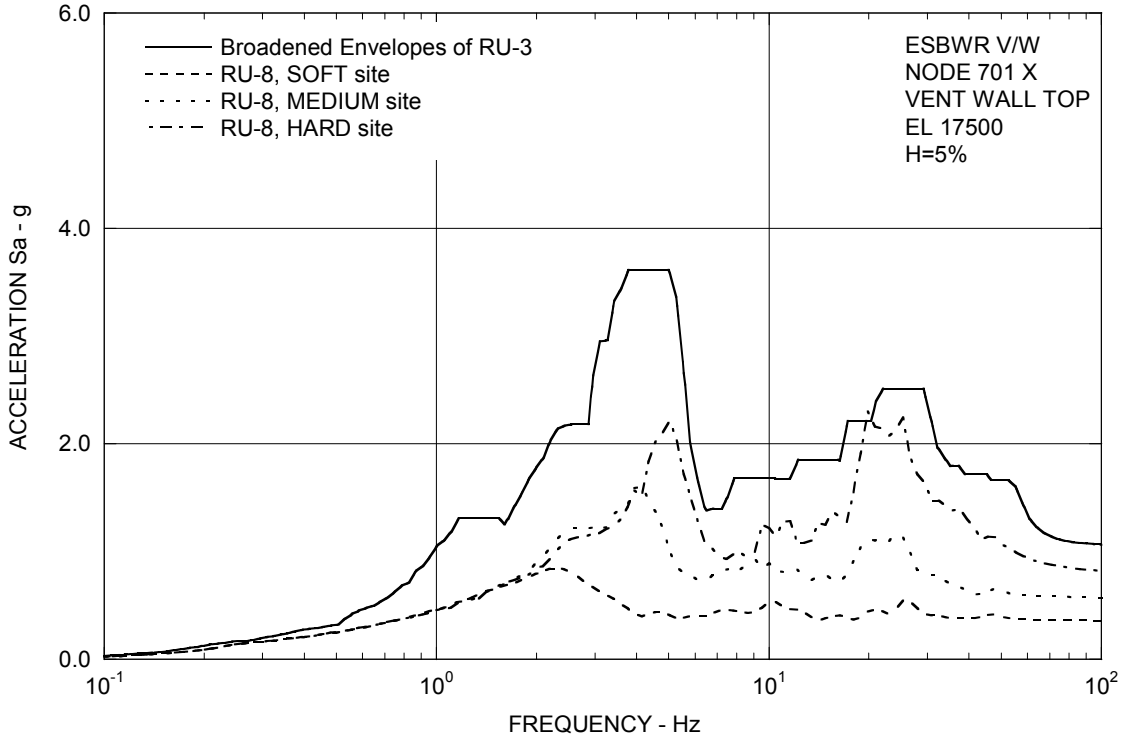

Figure 3.8-94(6) FRS (Compared with the DAC3N) – Vent Wall Top X

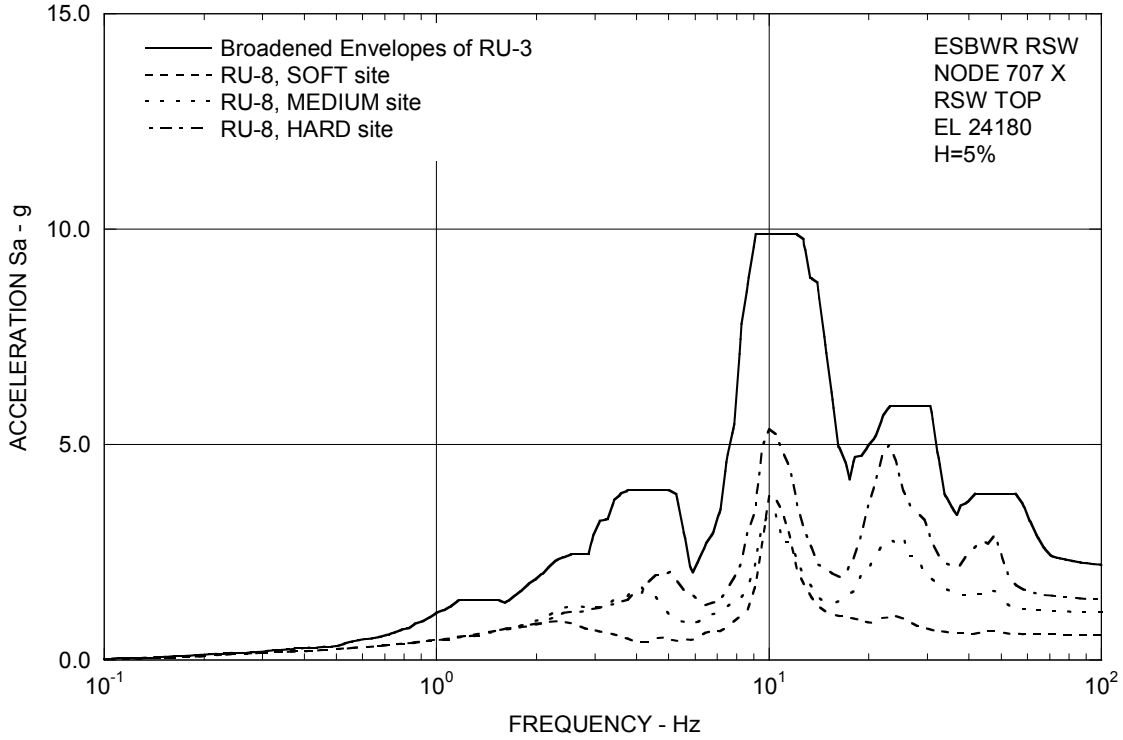

Figure 3.8-94(7) FRS (Compared with the DAC3N) – RSW Top X

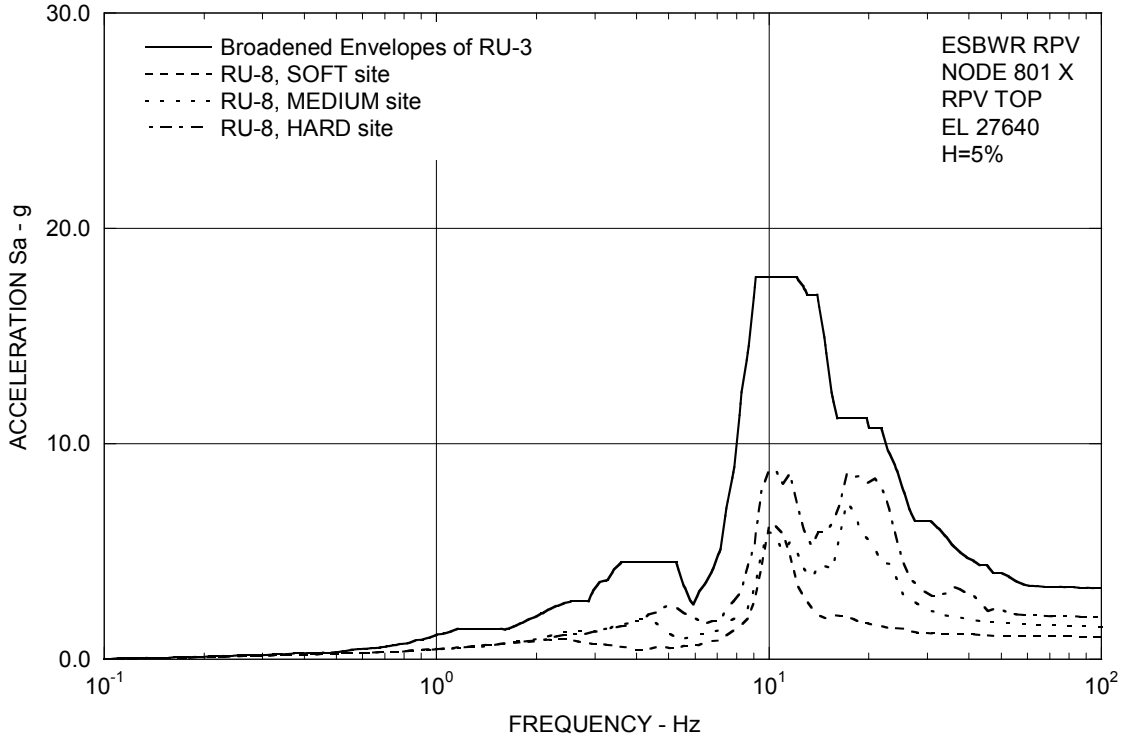

Figure 3.8-94(8) FRS (Compared with the DAC3N) – RPV Top X

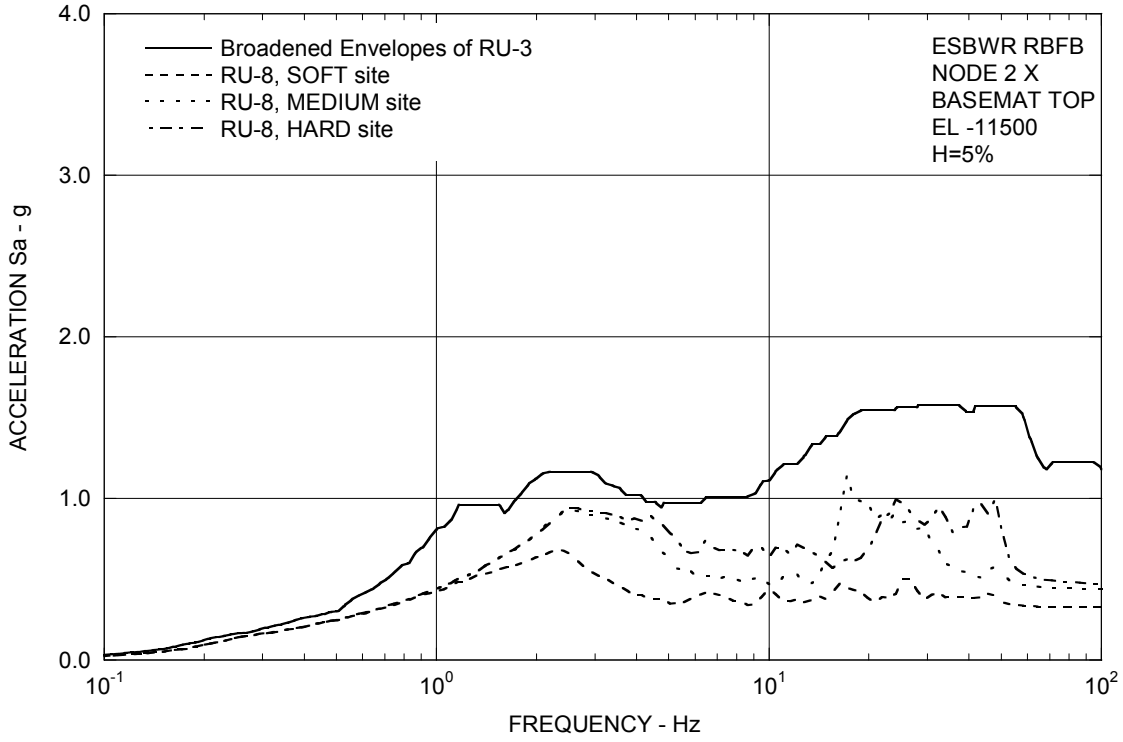

Figure 3.8-94(9) FRS (Compared with the DAC3N) – RBFB Basemat X

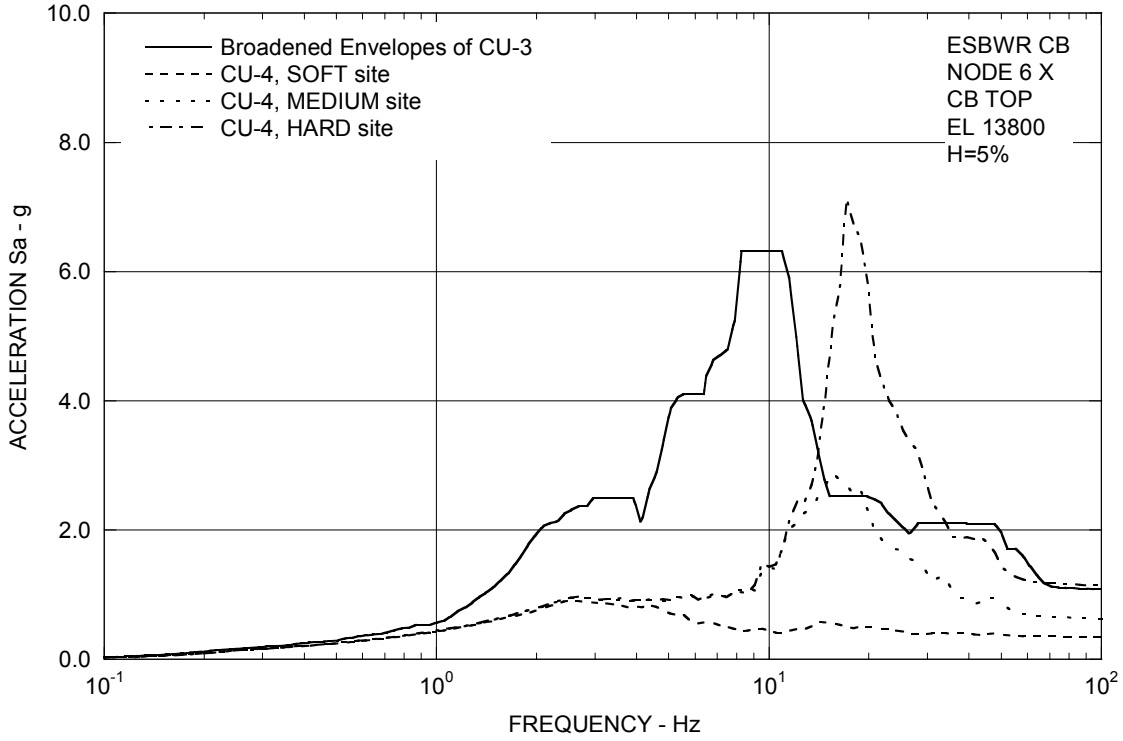

Figure 3.8-94(10) FRS (Compared with the DAC3N) – CB Top X

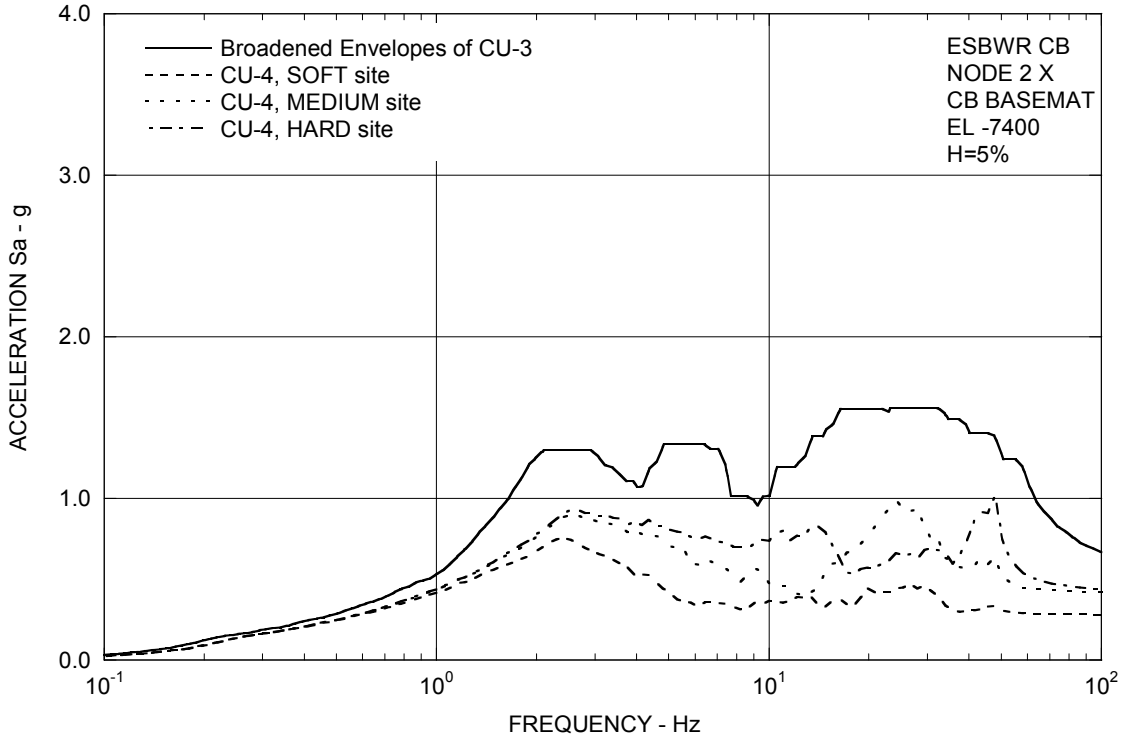

Figure 3.8-94(11) FRS (Compared with the DAC3N) – CB Basemat X

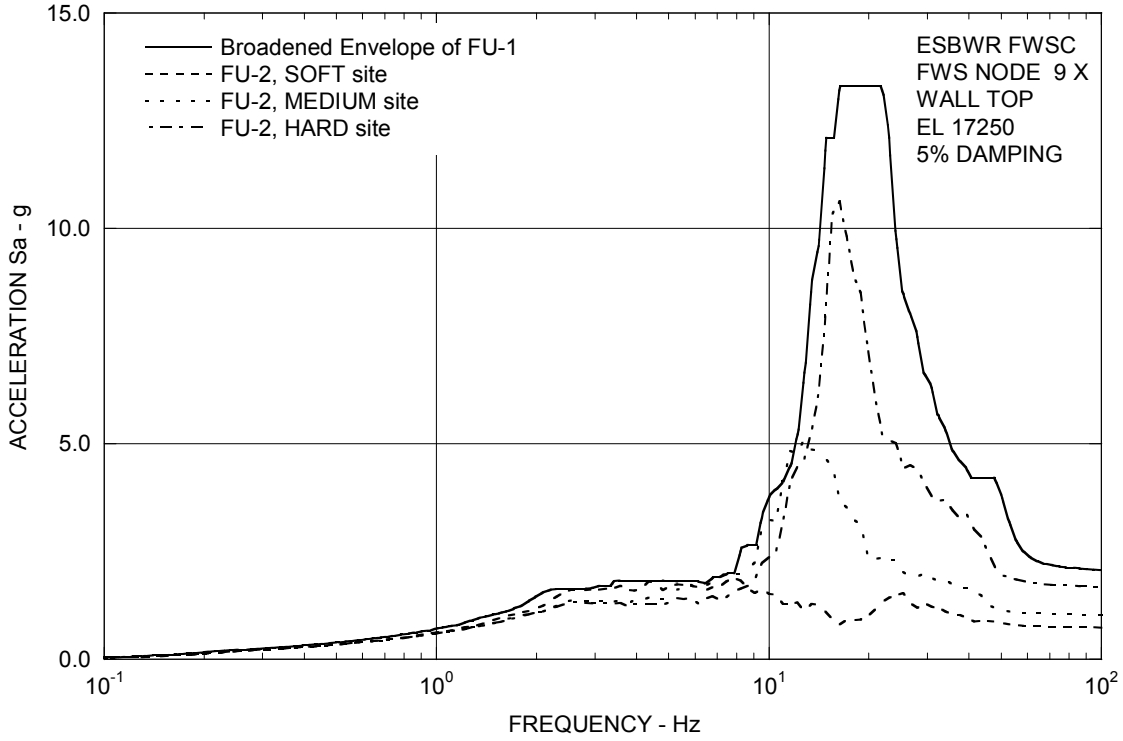

Figure 3.8-94(12) FRS (Compared with the DAC3N) – FWS Wall Top X

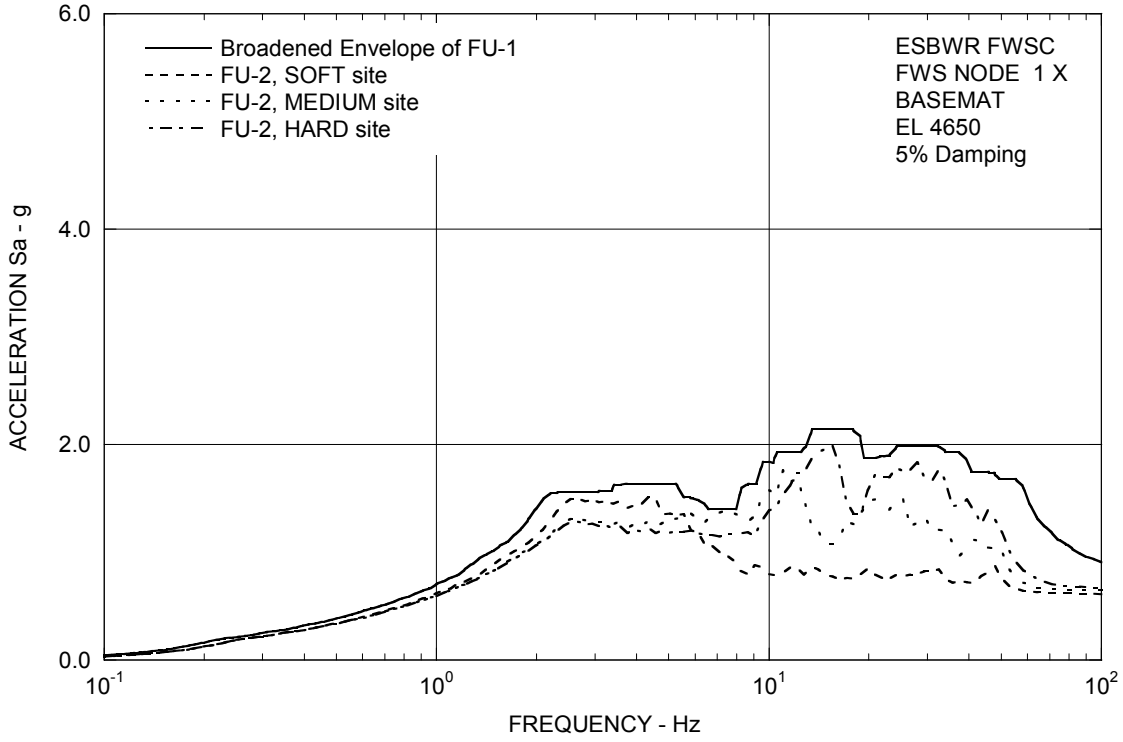

Figure 3.8-94(13) FRS (Compared with the DAC3N) – FWS Basemat X

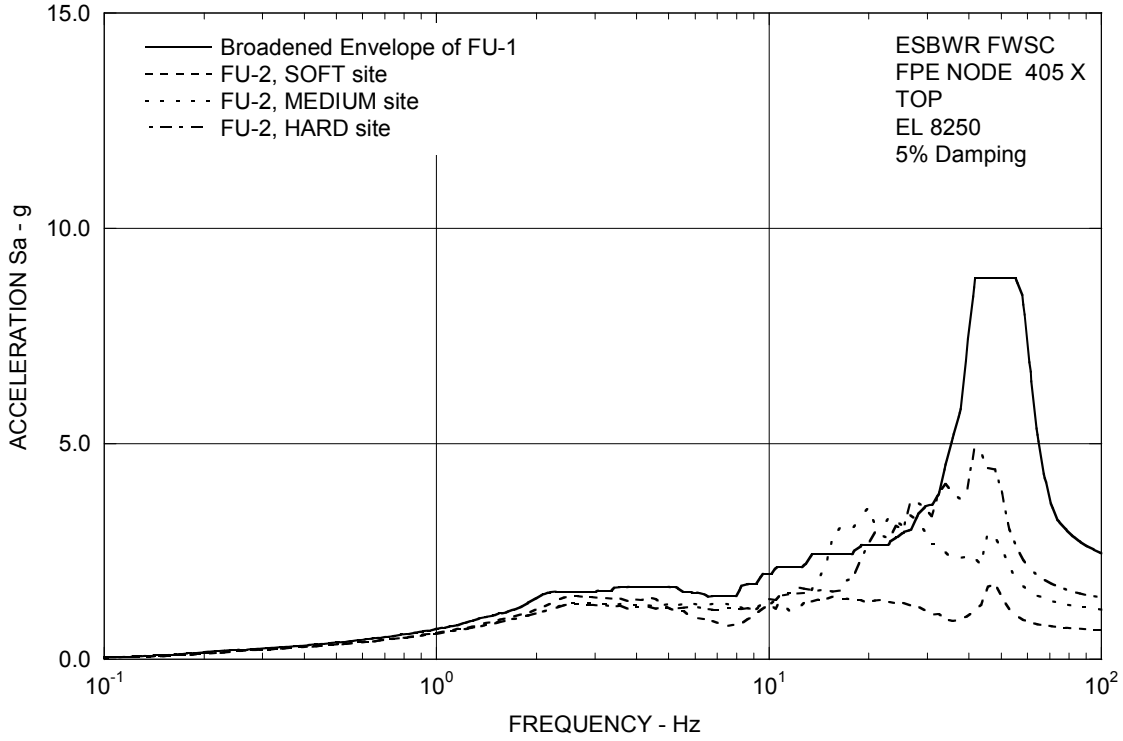

Figure 3.8-94(14) FRS (Compared with the DAC3N) – FPE Top X

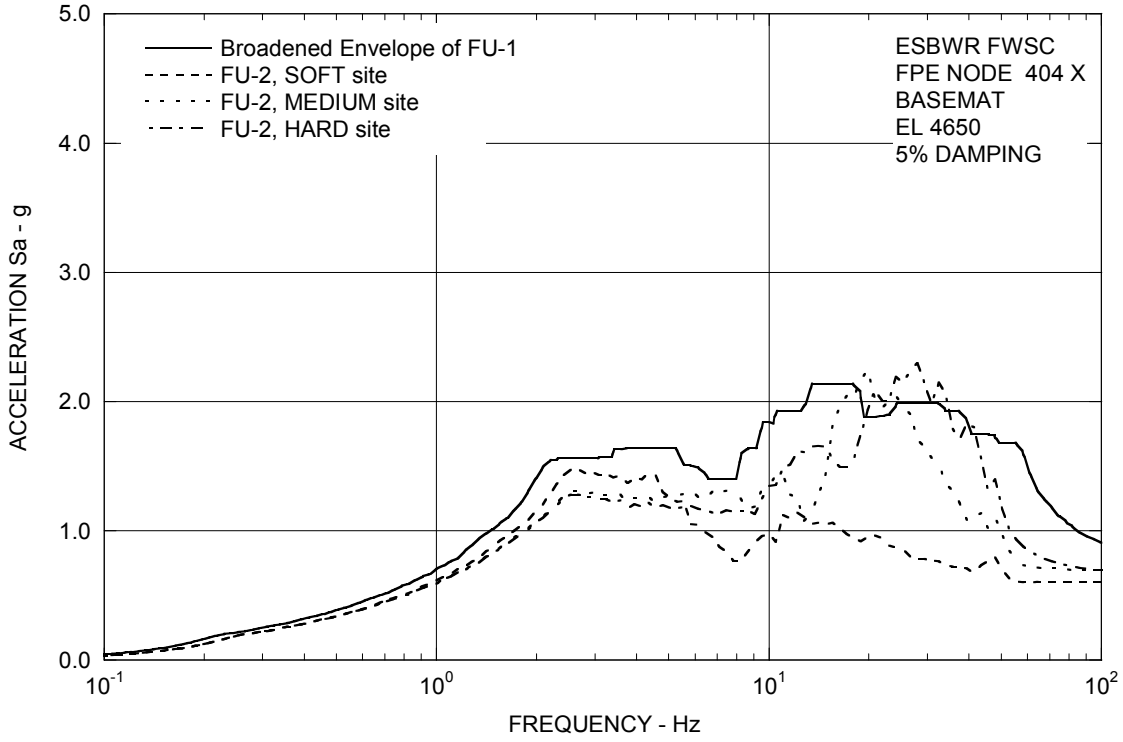

Figure 3.8-94(15) FRS (Compared with the DAC3N) – FPE Basemat X

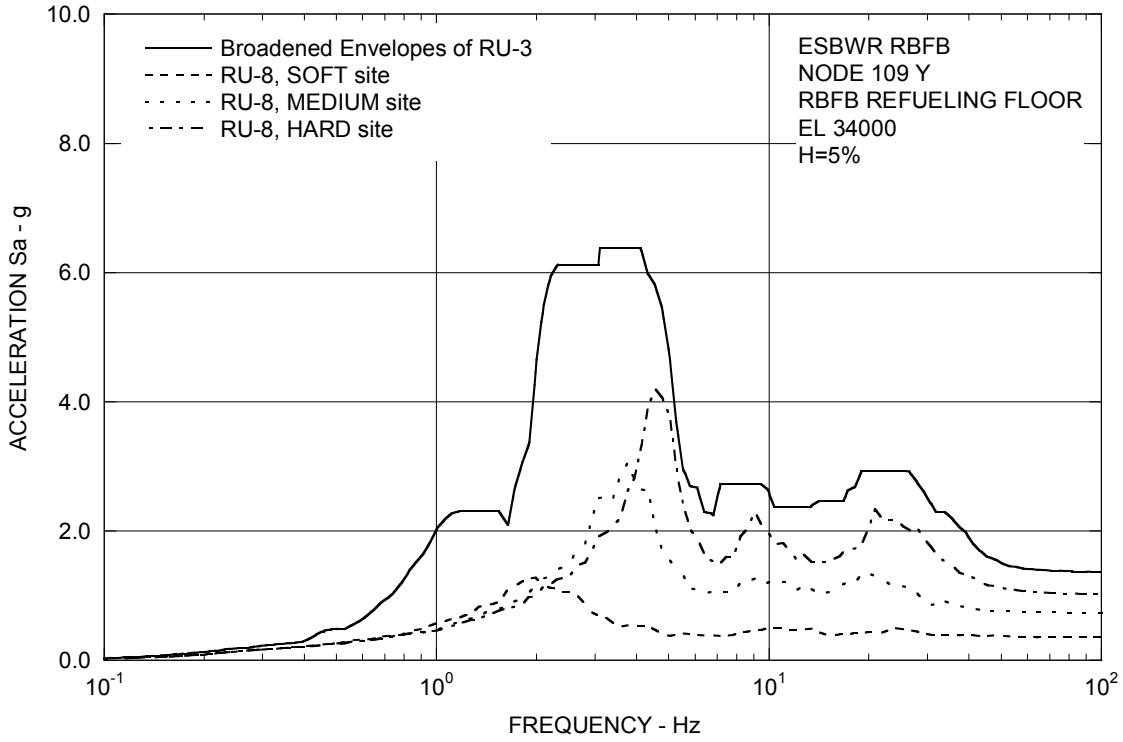

Figure 3.8-94(16) FRS (Compared with the DAC3N) – RBFB Refueling Floor Y

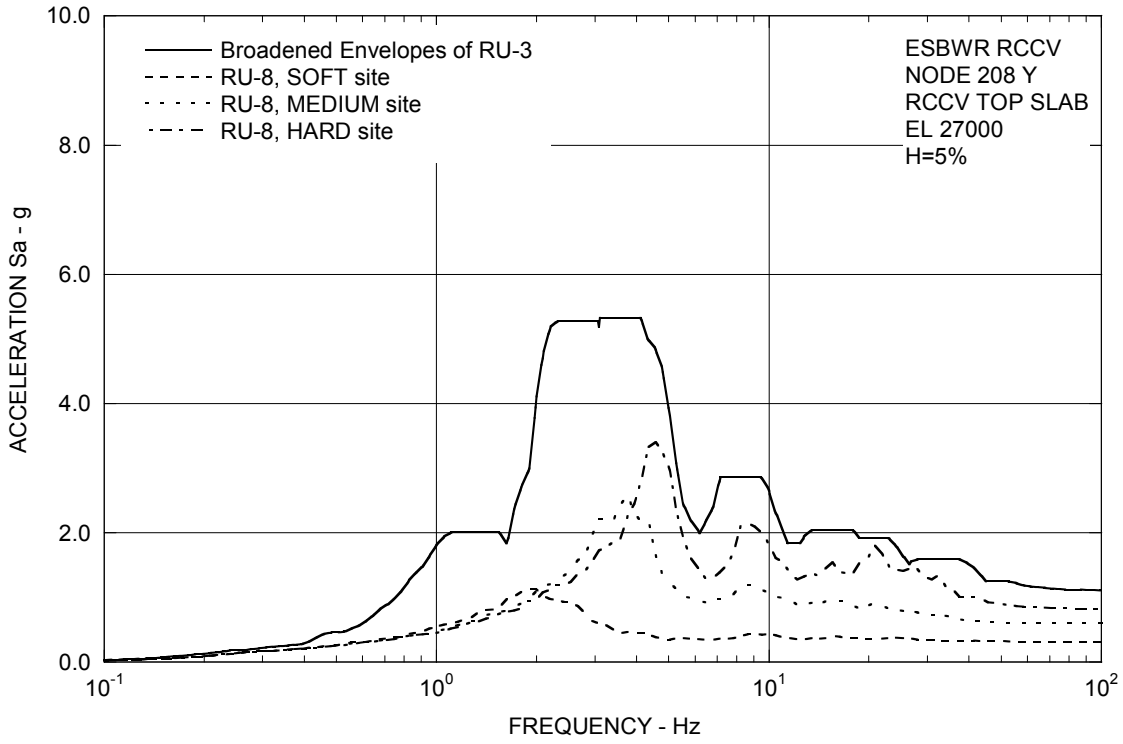

Figure 3.8-94(17) FRS (Compared with the DAC3N) – RCCV Top Slab Y

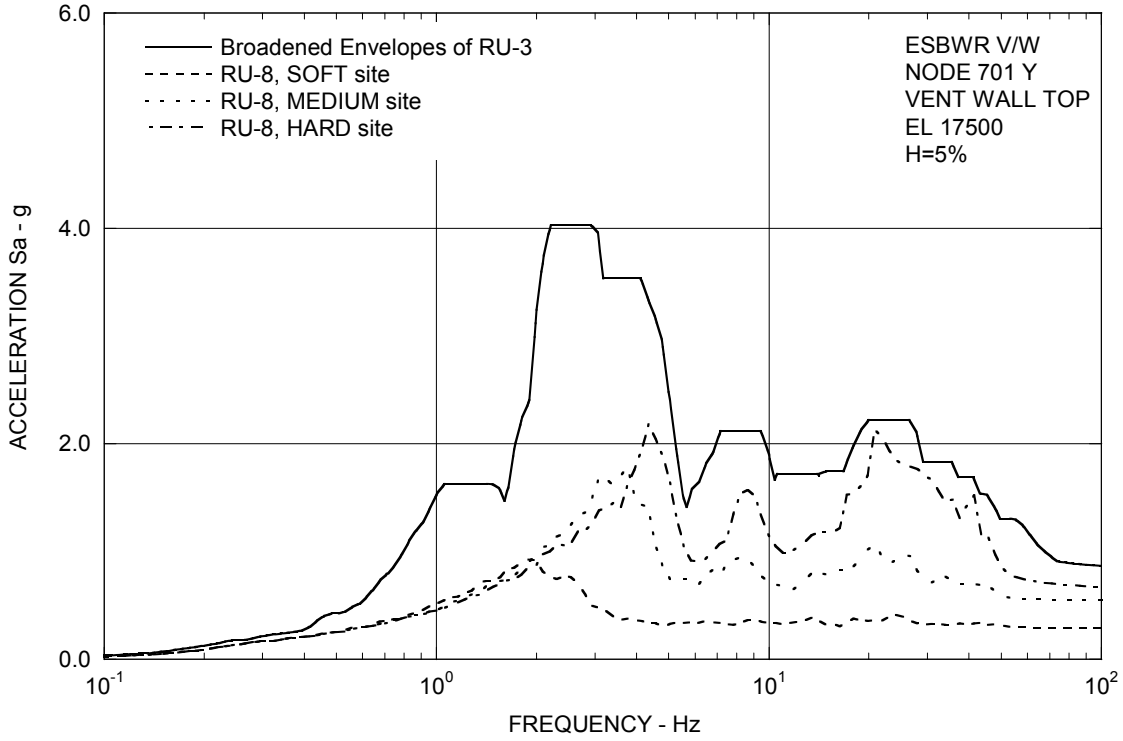

Figure 3.8-94(18) FRS (Compared with the DAC3N) – Vent Wall Top Y

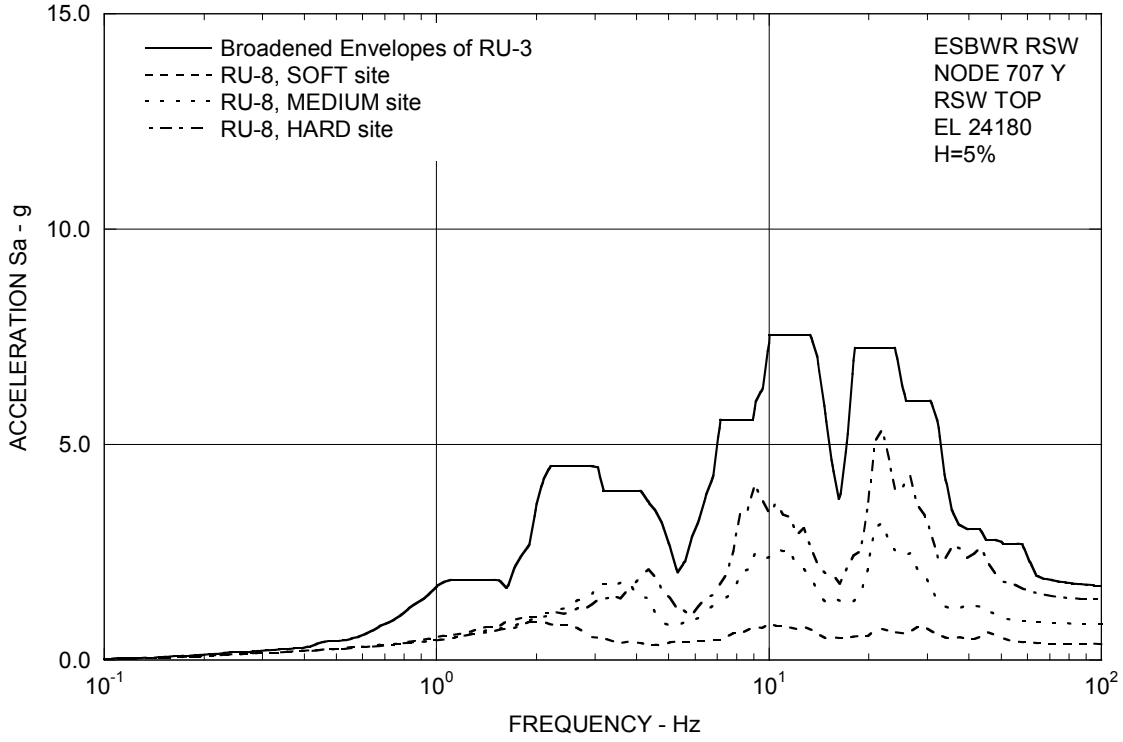

Figure 3.8-94(19) FRS (Compared with the DAC3N) – RSW Top Y

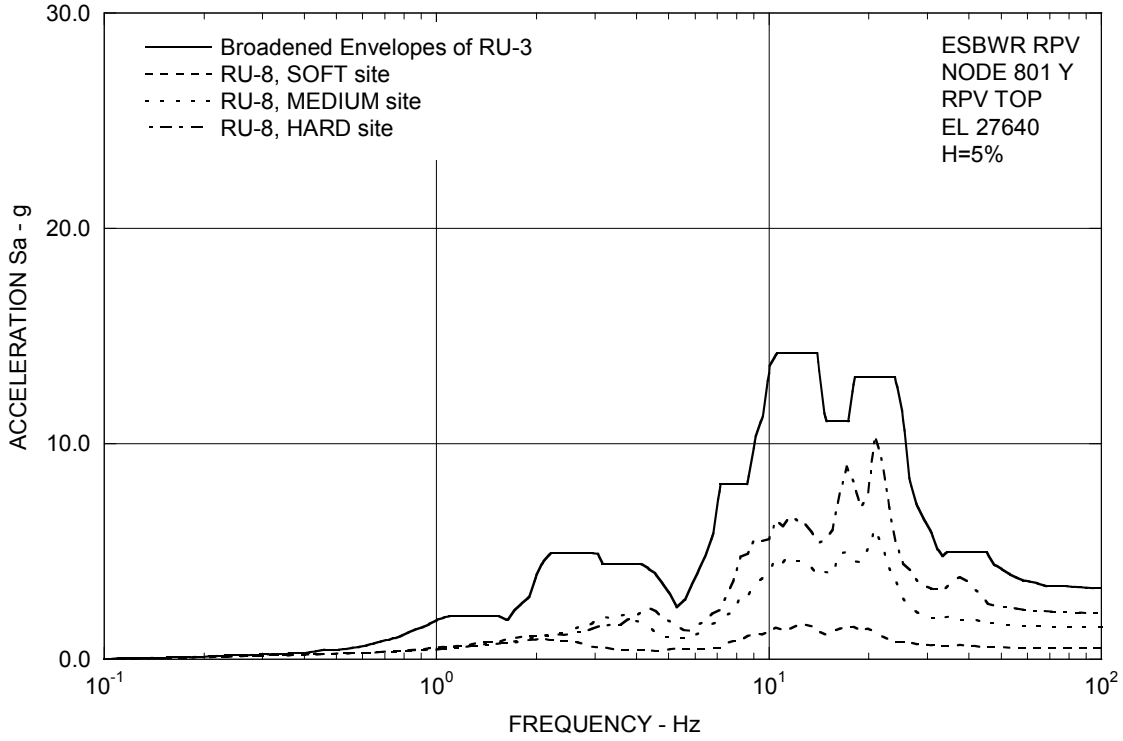

Figure 3.8-94(20) FRS (Compared with the DAC3N) – RPV Top Y

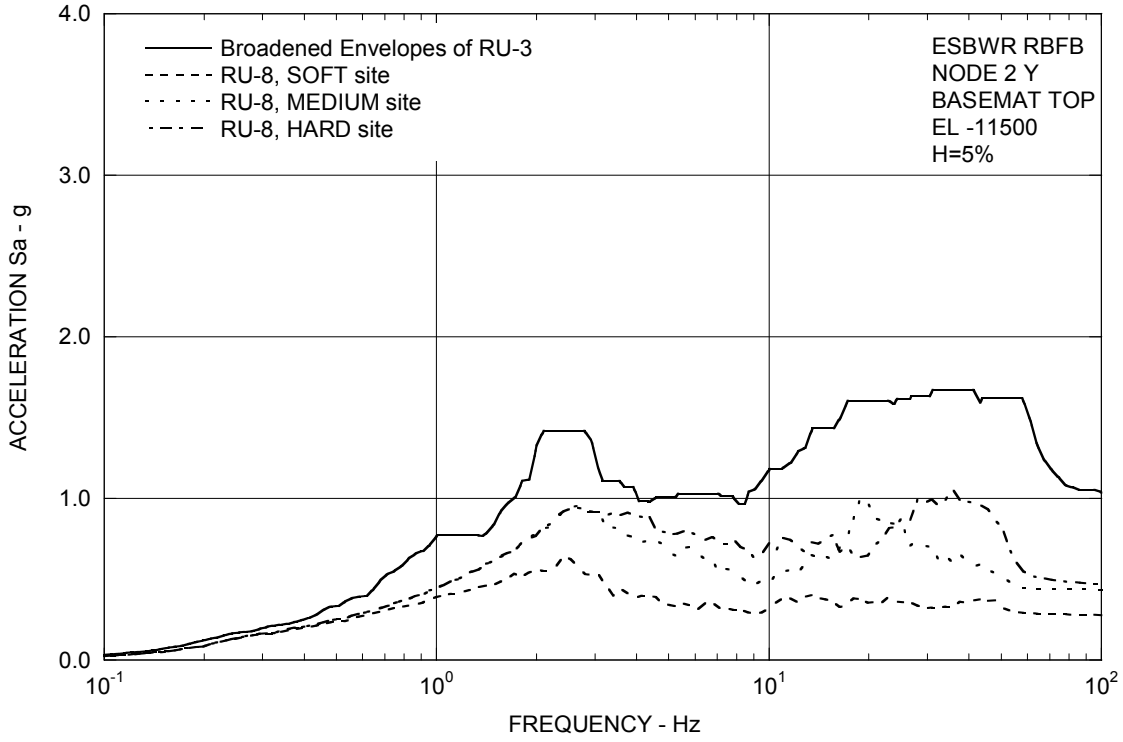

Figure 3.8-94(21) FRS (Compared with the DAC3N) – RBFB Basemat Y

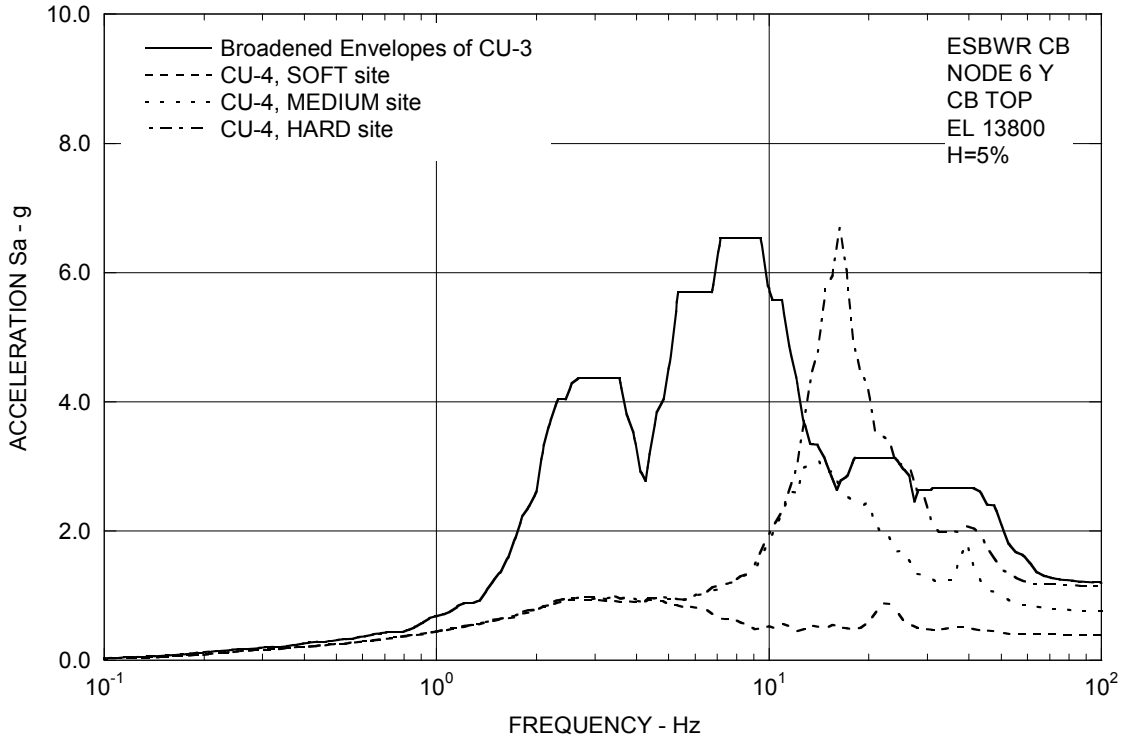

Figure 3.8-94(22) FRS (Compared with the DAC3N) – CB Top Y

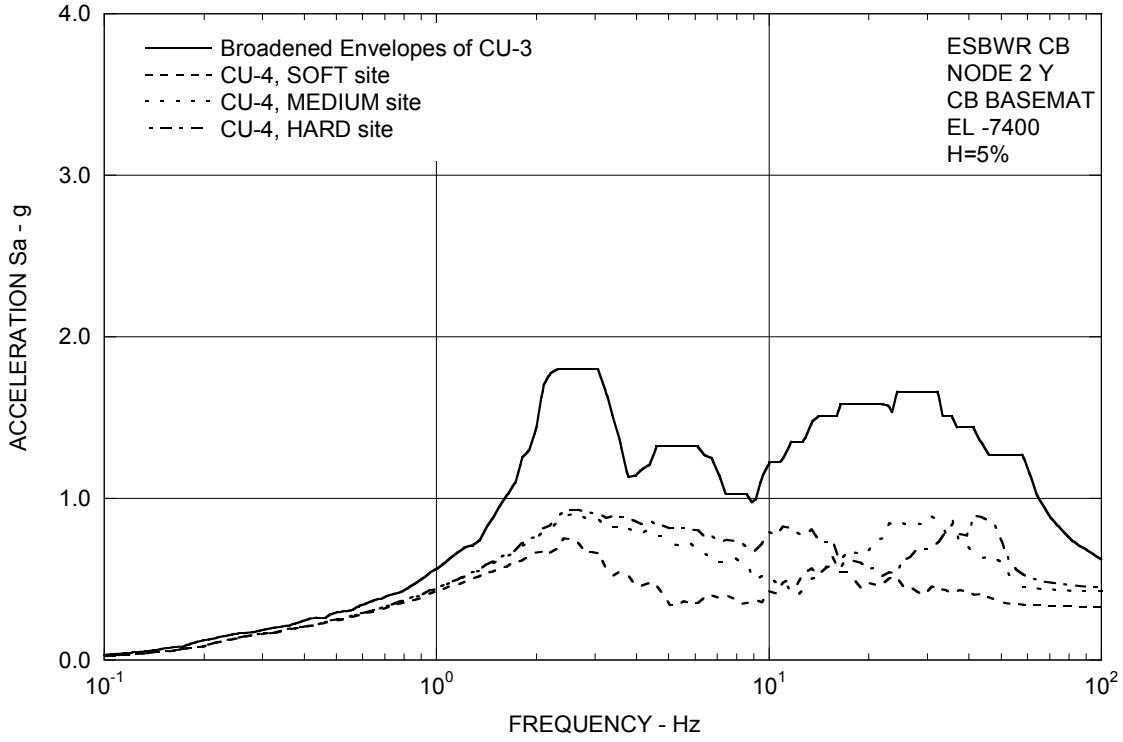

Figure 3.8-94(23) FRS (Compared with the DAC3N) – CB Basemat Y

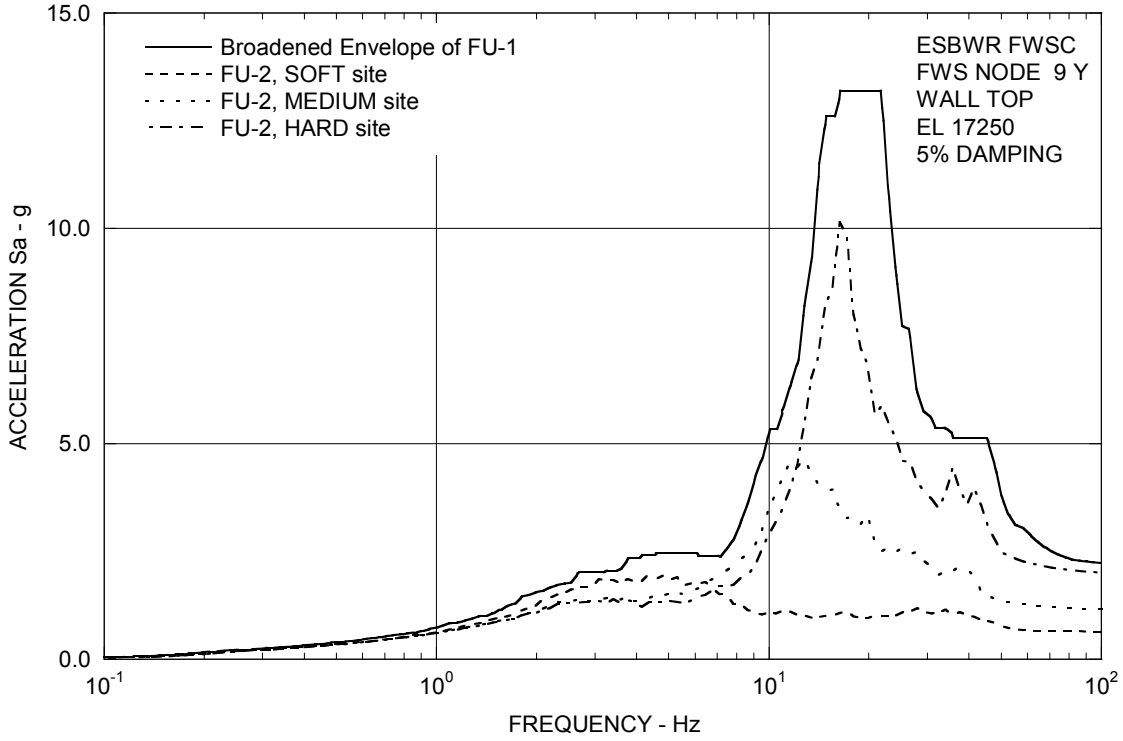

Figure 3.8-94(24) FRS (Compared with the DAC3N) – FWS Wall Top Y

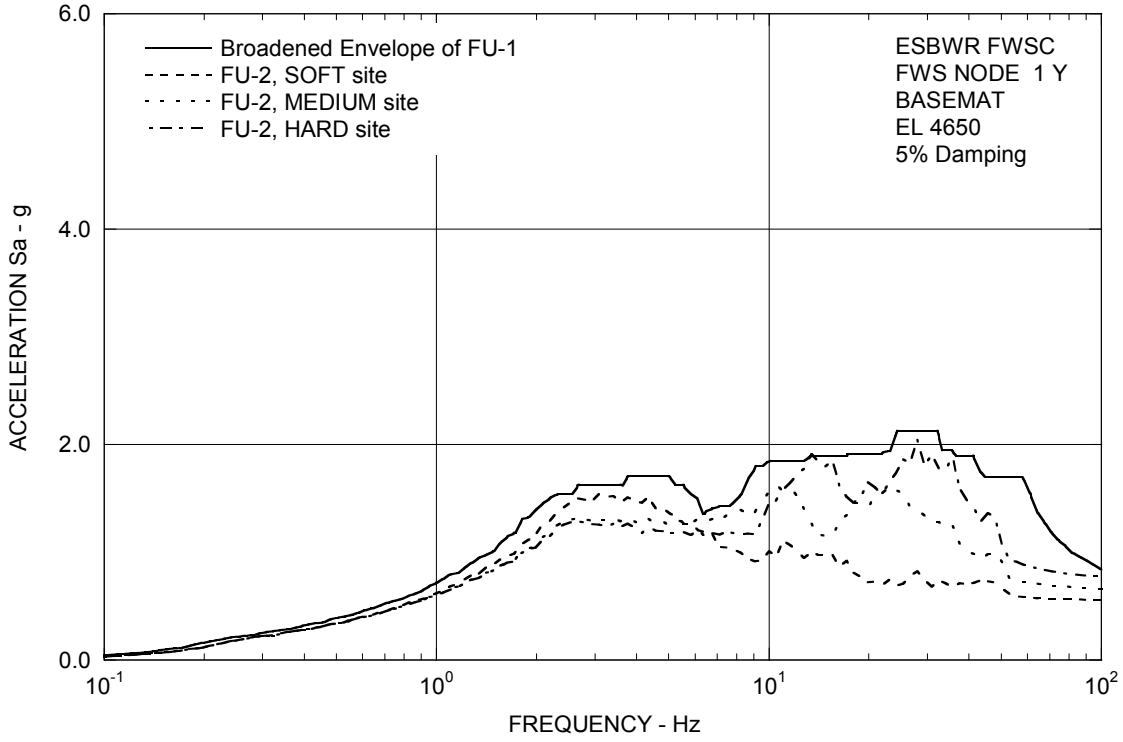

Figure 3.8-94(25) FRS (Compared with the DAC3N) – FWS Basemat Y

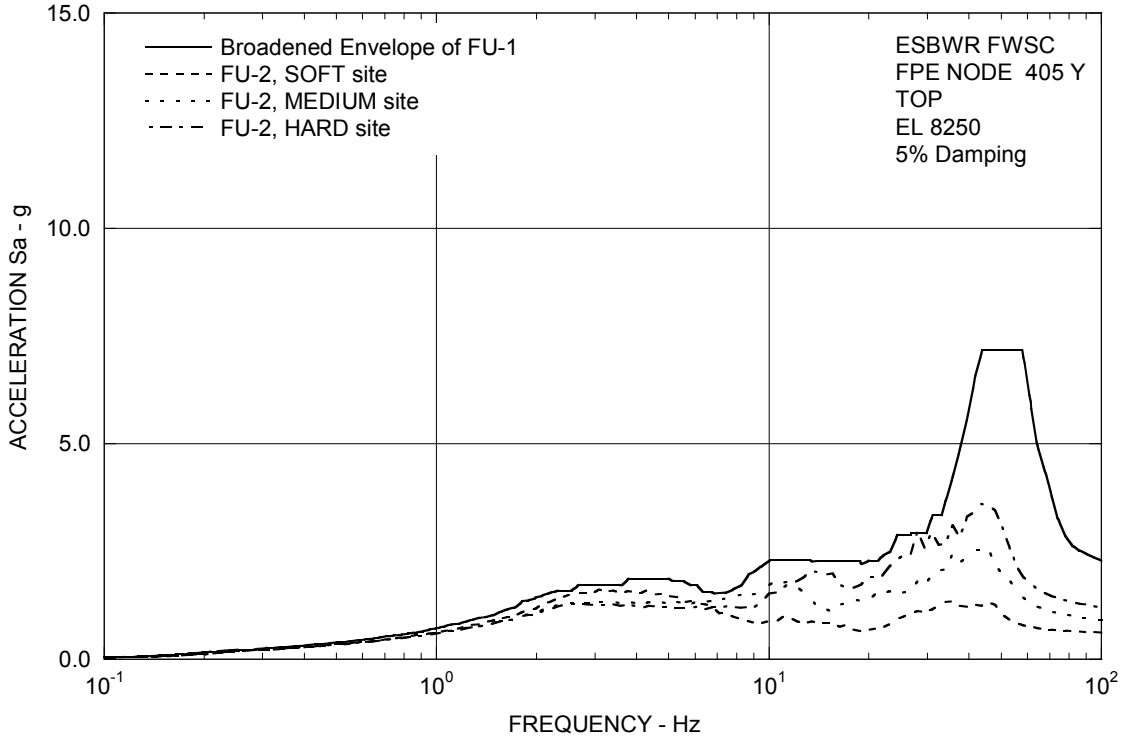

Figure 3.8-94(26) FRS (Compared with the DAC3N) – FPE Top Y

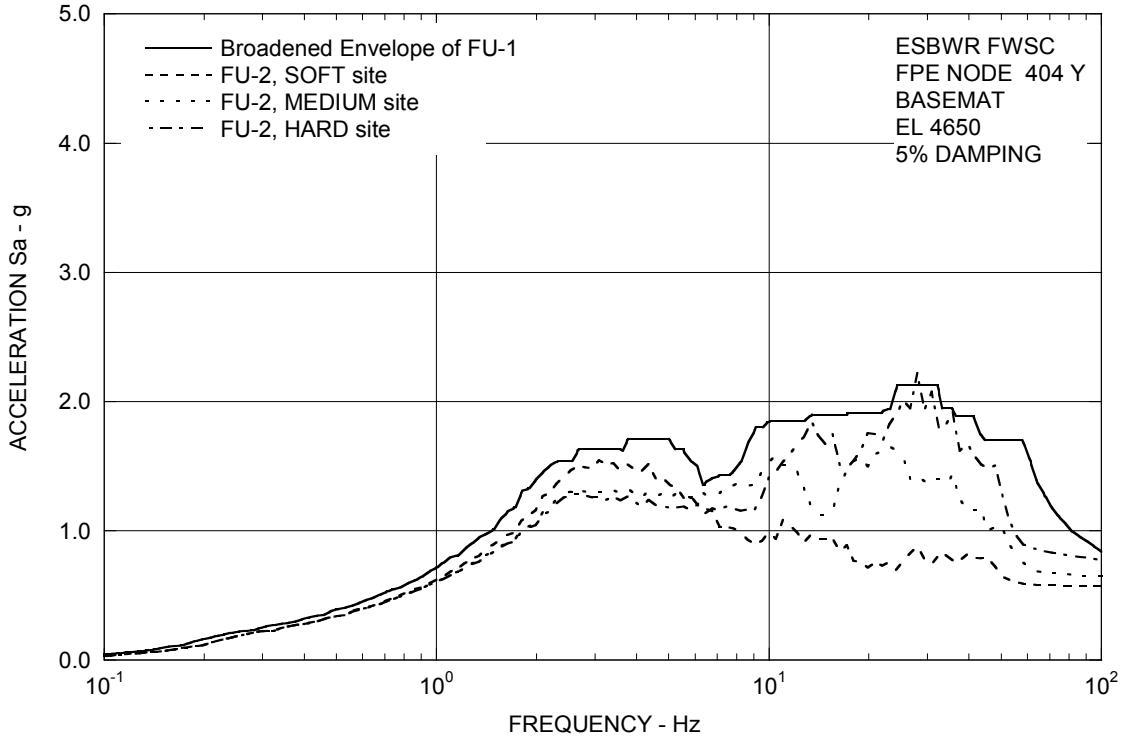

Figure 3.8-94(27) FRS (Compared with the DAC3N) – FPE Basemat Y

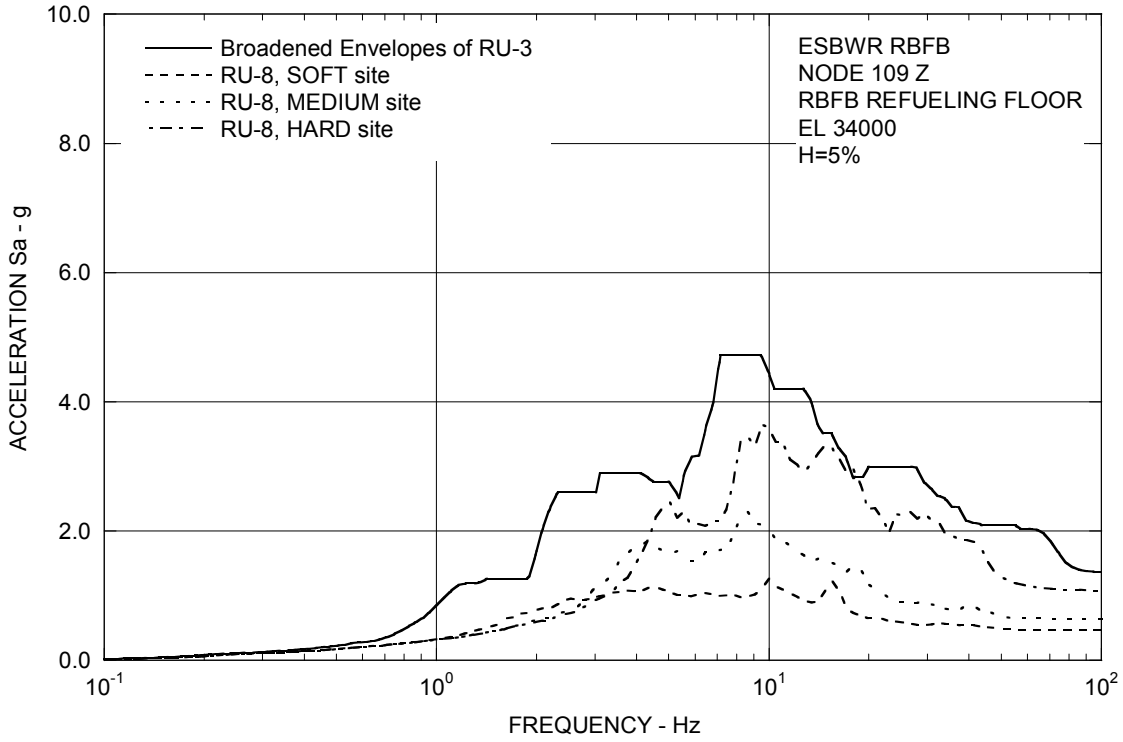

Figure 3.8-94(28) FRS (Compared with the DAC3N) – RBFB Refueling Floor Z

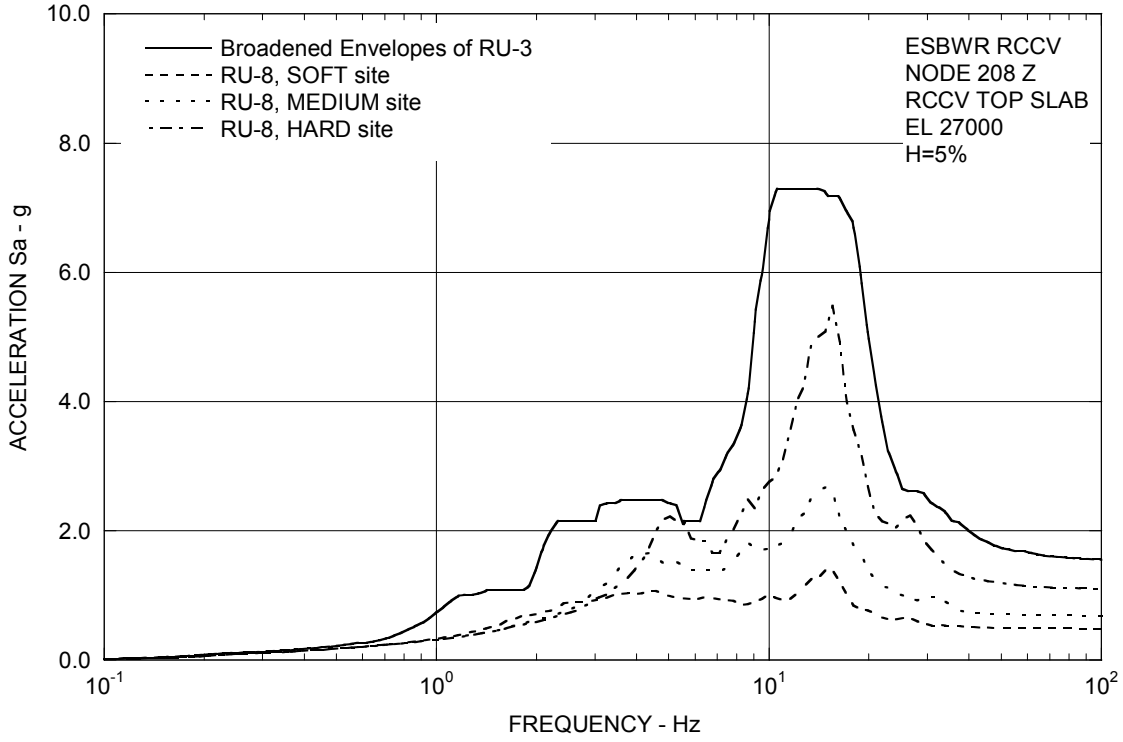

Figure 3.8-94(29) FRS (Compared with the DAC3N) – RCCV Top Slab Z

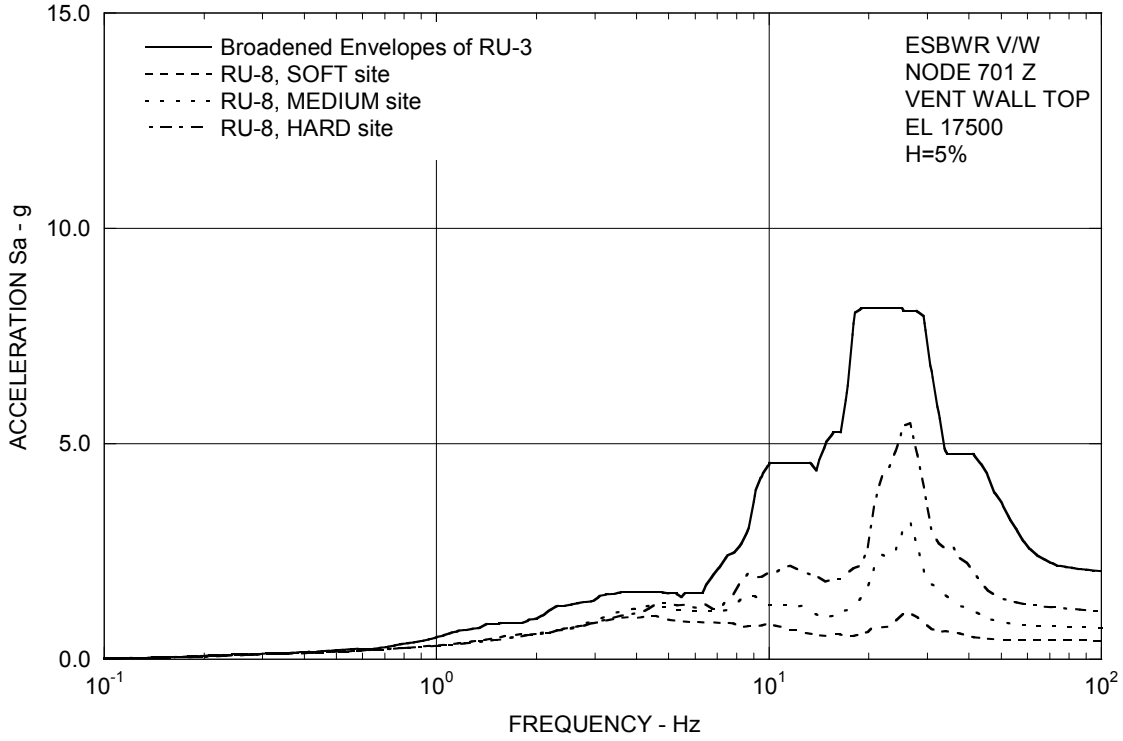

Figure 3.8-94(30) FRS (Compared with the DAC3N) – Vent Wall Top Z

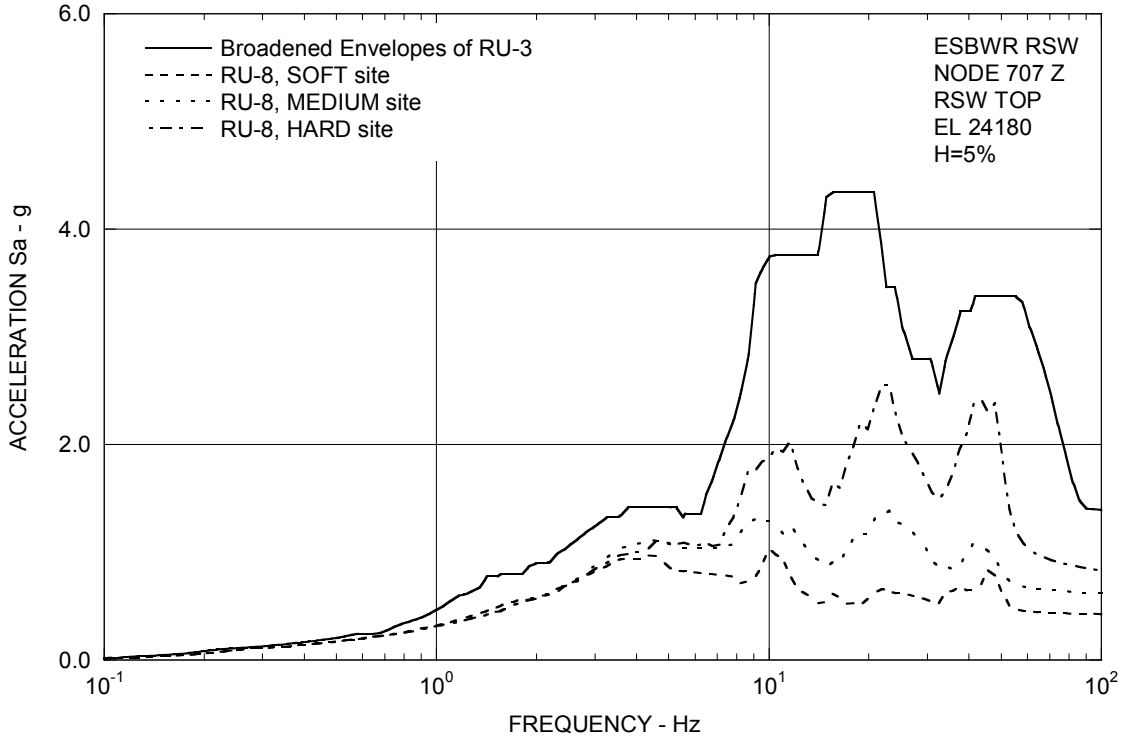

Figure 3.8-94(31) FRS (Compared with the DAC3N) – RSW Top Z

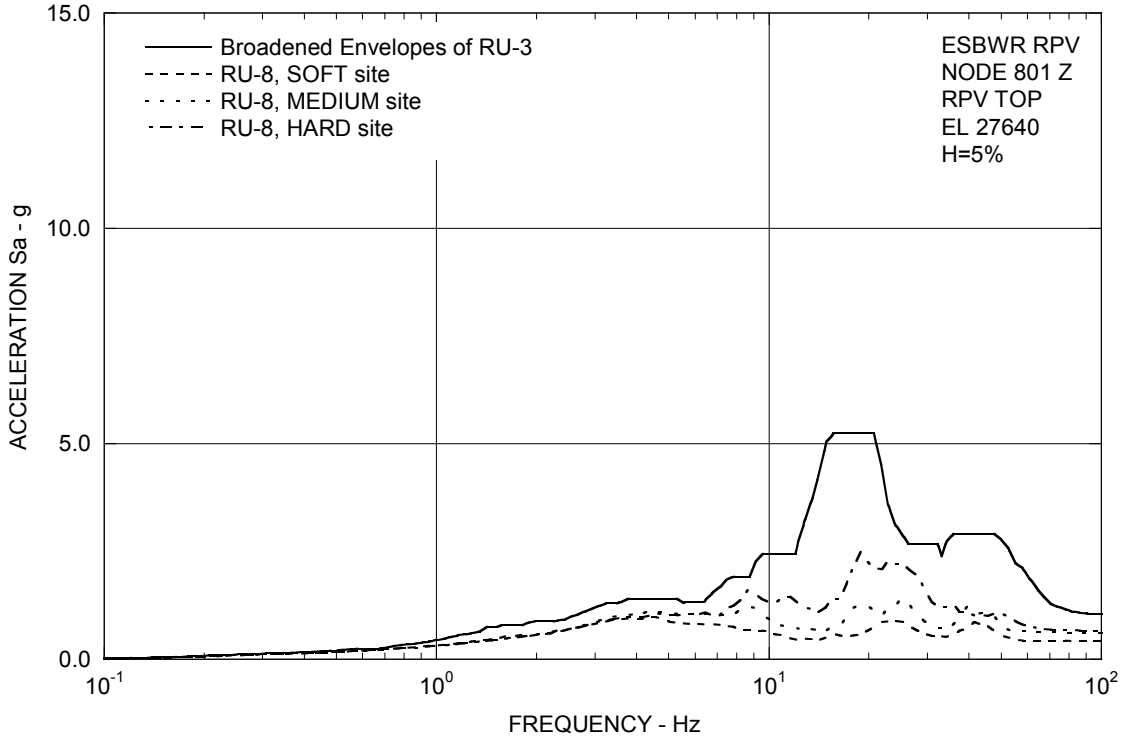

Figure 3.8-94(32) FRS (Compared with the DAC3N) – RPV Top Z

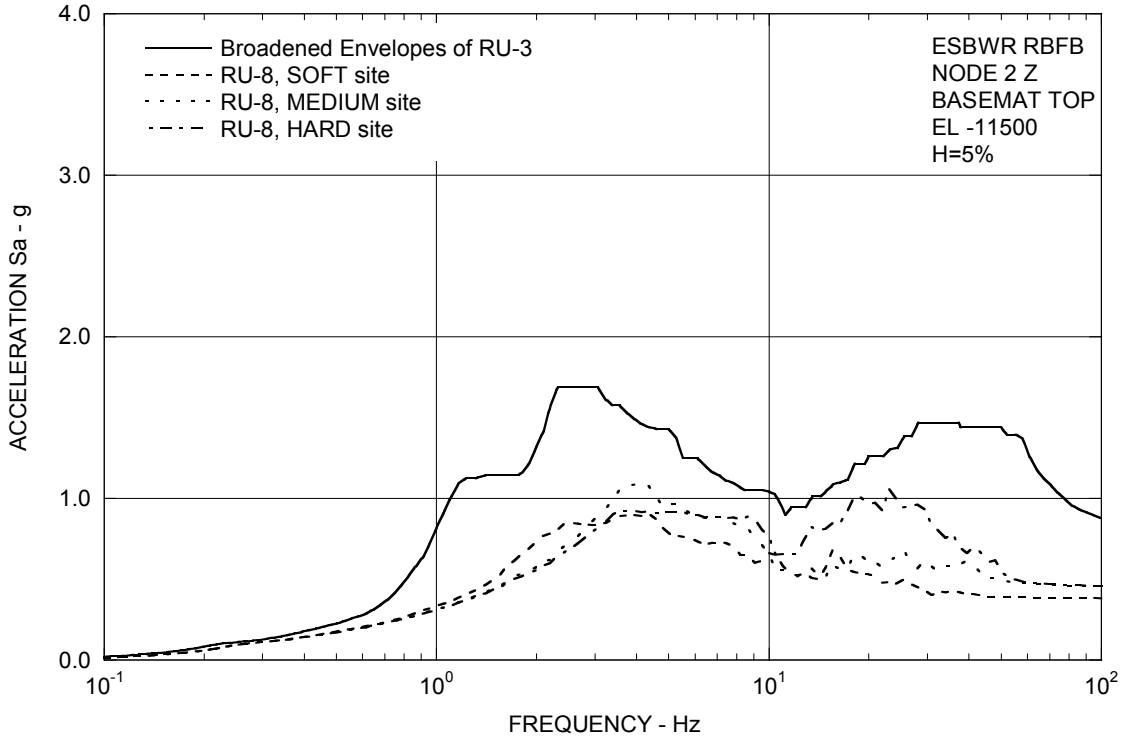

Figure 3.8-94(33) FRS (Compared with the DAC3N) – RBFB Basemat Z

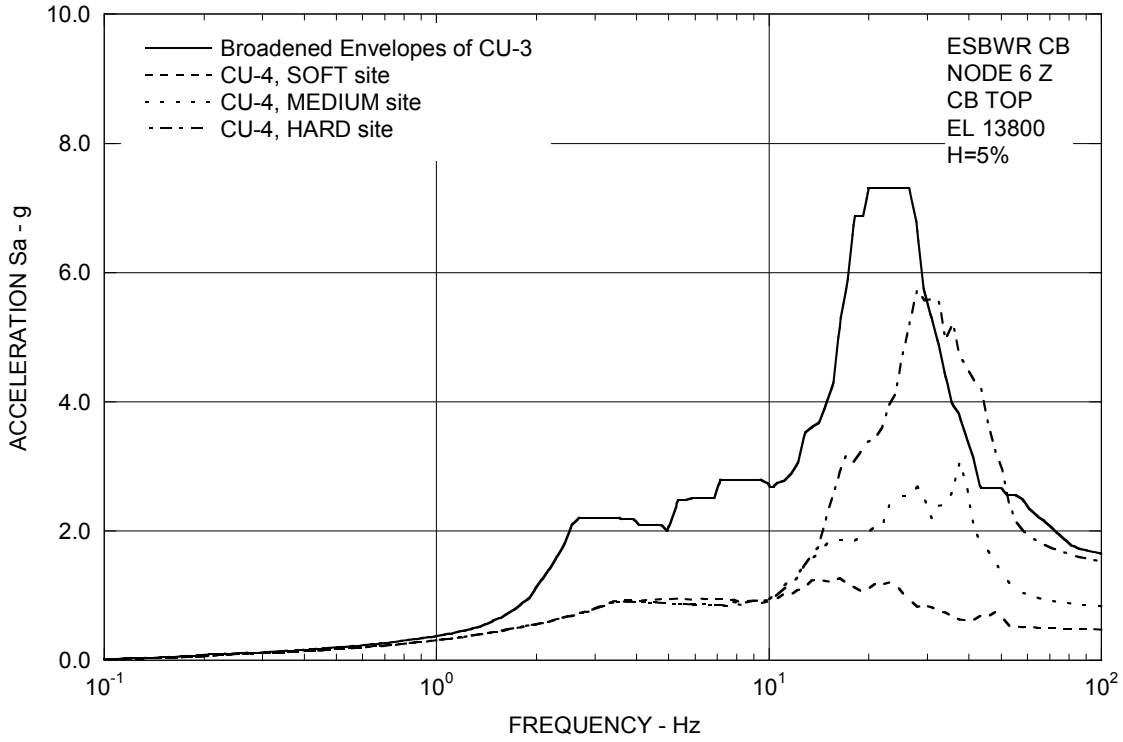

Figure 3.8-94(34) FRS (Compared with the DAC3N) – CB Top Z

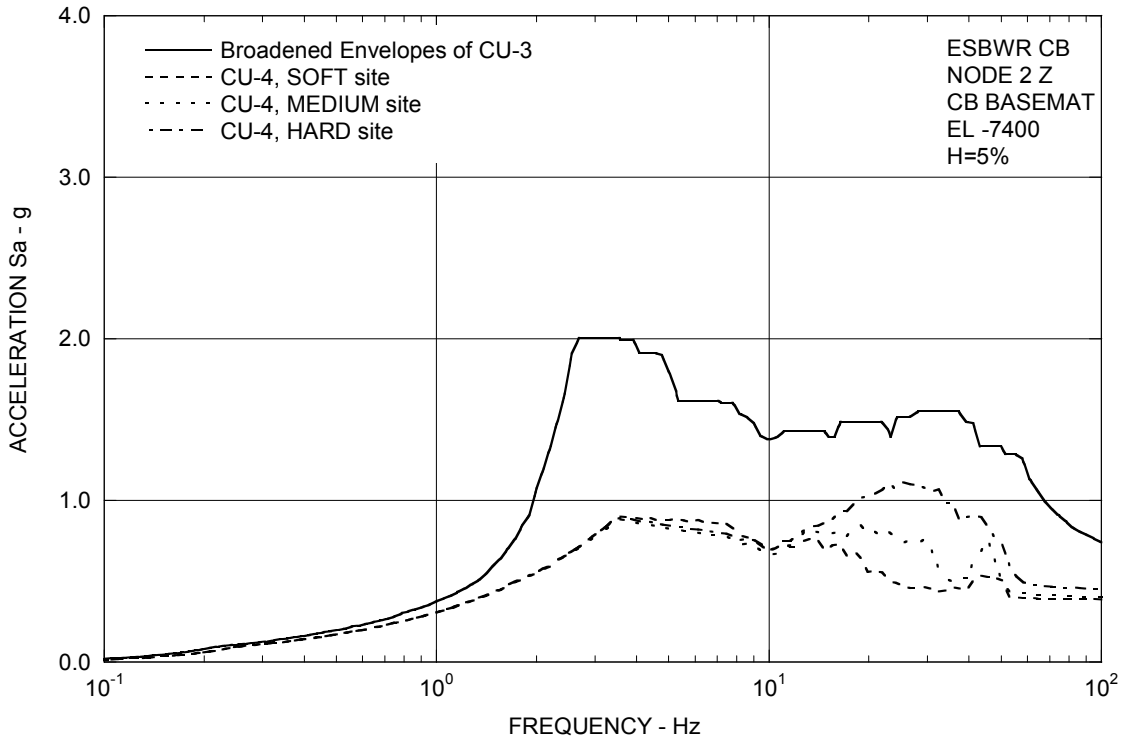

Figure 3.8-94(35) FRS (Compared with the DAC3N) – CB Basemat Z

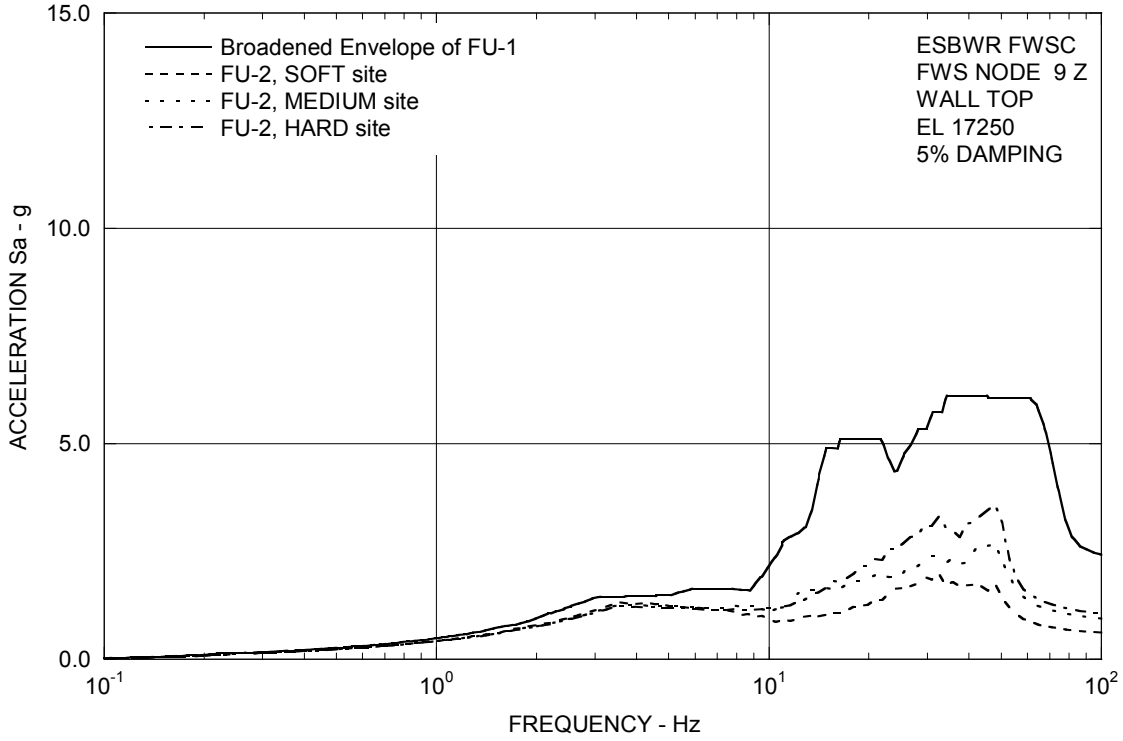

Figure 3.8-94(36) FRS (Compared with the DAC3N) – FWS Wall Top Z

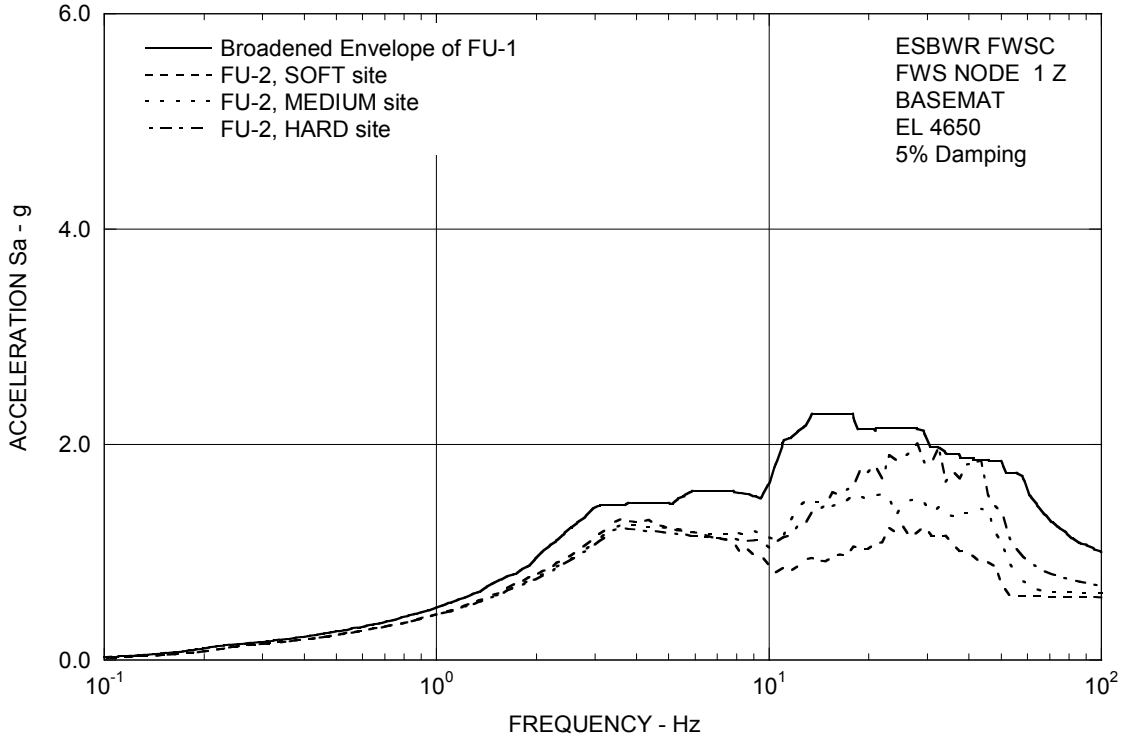

Figure 3.8-94(37) FRS (Compared with the DAC3N) – FWS Basemat Z

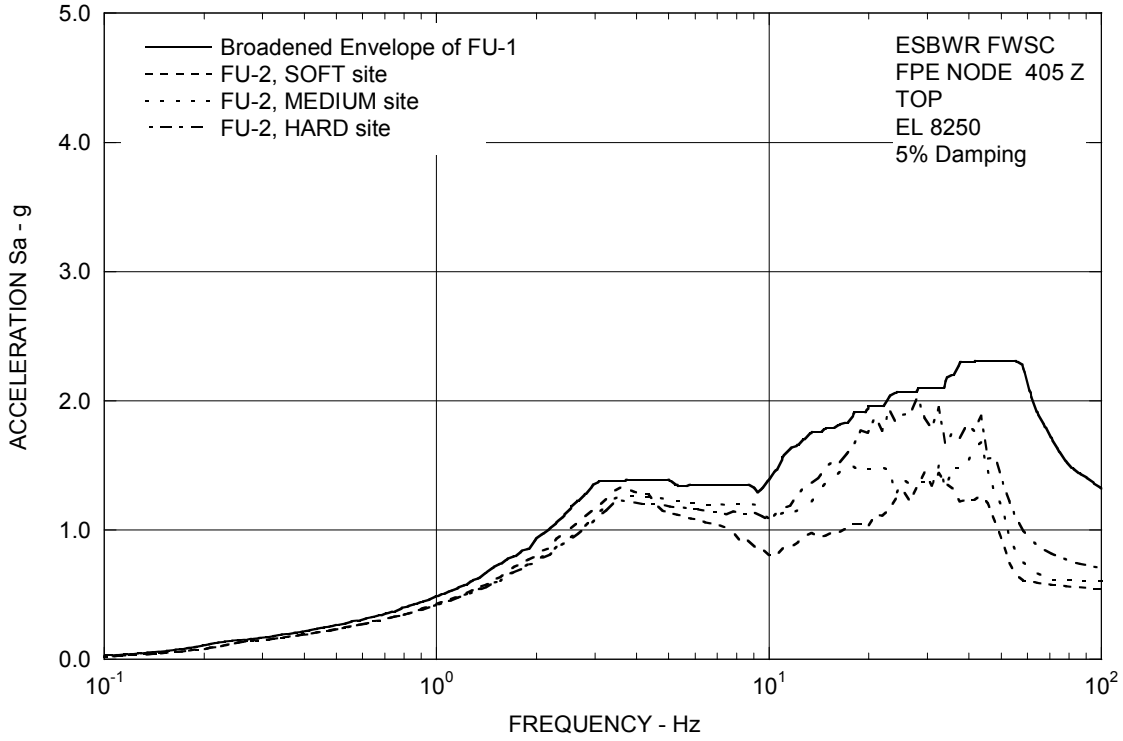

Figure 3.8-94(38) FRS (Compared with the DAC3N) – FPE Top Z

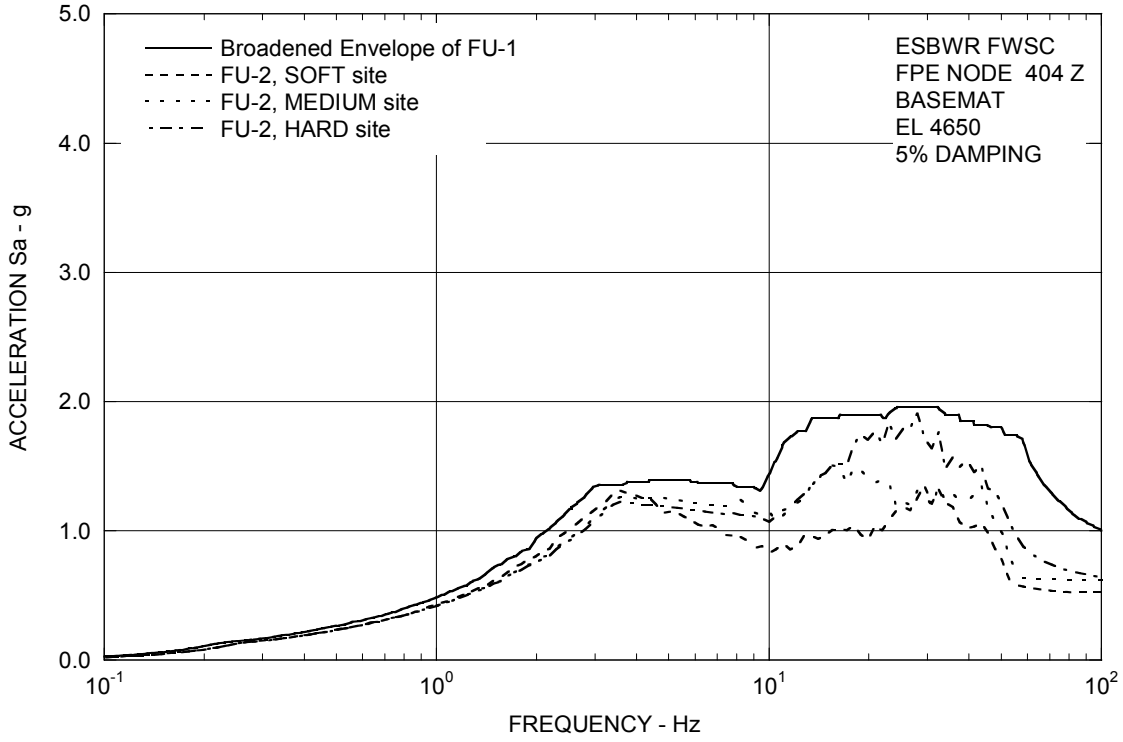

Figure 3.8-94(39) FRS (Compared with the DAC3N) – FPE Basemat Z

DCD Impact

Markups of DCD Tier 1 Table 5.1-1, DCD Tier 2 Subsections 3.7.1.1.3, 3A.5, 3A.5.2, 3A.6, 3A.8.7, 3A.9.3, 3C.7.1.3, 3C.7.2.1 and 3C.7.2.3, Tables 2.0-1, 3.7-3, 3A.6-1, 3A.8.7-1, 3G.1-58, 3G.2-27 and 3G.4-23 and Figures 3A.8.7-1a through 3A.8.7-1l, 3A.8.7-2a through 3A.8.7-2l, 3A.8.7-3a through 3A.8.7-3l, 3A.9-1g, 3A.9-1l, 3A.9-2g and 3A.9-3g were provided to the NRC in MFN 06-407 S13, dated 2/20/09.

NRC RAI 3.8-94, Supplement 4

Based on the review of GEH RAI 3.8-94 S03 response, presented in GEH letter dated February 20, 2009, GEH is requested to address the items described below.

A) As described on page 10 of 34 in the RAI response, the evaluation of peak toe pressure is made considering the bearing pressures due to the three perpendicular earthquake directions at only three time steps and not at every time step throughout the time history. The three time steps correspond to the time when Mx is maximum, when My is maximum, and when V is maximum. At each of these three time steps, the other two corresponding forces are utilized. GEH is requested to provide the technical basis why this approach is considered to be acceptable since at other time steps, where Mx, My, and V may not be maximum values, the resulting bearing pressures may actually be higher. Typically, a bearing pressure time history analysis should be performed at every time steps using algebraic summation or alternatively, the bearing pressures due to the three maximum forces may be combined by the SRSS method.

B) As described on page 11 of 34 in the RAI response, the calculation of bearing pressure is performed for one horizontal and vertical directions (i.e., two dimensional evaluation) using the "Energy Balance Method." Then another calculation is performed for the maximum bearing pressure contribution from the other horizontal earthquake direction. The total bearing pressure is then determined by the addition of these two values. GEH is requested to describe and identify the source of the specific "Energy Balance Method" being used to calculate the bearing pressure for this evaluation. Also, explain how the contact lengths CL and CW shown on page 10 of 33 are determined.

C) The forces used to calculate the maximum soil bearing pressures were obtained from the SASSI analyses. These analyses consider that the soil and foundation are integrally connected. However, the bearing pressure calculations on page 11 of 34 show that uplift occurs. Describe the extent of the maximum uplift that occurs in SASSI (denoted by tension in the soil springs), recognizing that this region could expand further if the tension springs would be released using a different computer code. Provide the technical basis for using these seismic loads in the bearing and sliding calculations from the SASSI analyses without consideration of the effects of uplift on the seismic demand loadings. Alternatively, an analysis that considers the nonlinear effect of liftoff due to the three input directions applied simultaneously can be considered.

D) In Item 3 on page 12 of 34 (Evaluation of Results), GEH indicates that the resulting toe pressures from the two layered soil cases (L2 and L4) are large as compared to those of the other generic soil cases. GEH deduces that this result may be due to the fact that large velocity contrasts exist in the layers of these cases (greater than 2.5). In the last paragraph on this page, the statement is made that "the best estimate low strain profile can be used because only the velocity ratio is of interest". However, it is not clear if this difference is in fact the only cause or even the primary

cause of the computed large peak responses. Other issues (such as the reduction in site radiation damping due to layering effects, ratios of the velocity to the bedrock velocities below, impact of layer thickness on the computed site amplification, etc.) may in fact contribute to such large responses. Provide detailed information to indicate that (a) the velocity ratio is the primary parameter controlling such high amplifications in toe pressure, and (b) the value of the site parameters that will lead to acceptable levels of peak toe pressure. Also see requested information in the new RAIs 3.7-70 and 71, which relate to this issue.

E) *In the same discussion (Item 3 on page 12 of 34 - Evaluation of Results), a new site interface parameter, for the maximum ratio of soil shear wave velocity in adjacent layers, will be added to the DCD. The RAI response states that "The ratio is the average velocity of the bottom layer divided by the average velocity of the top layer." Provide a description of how the average shear wave velocity is calculated and include it in the appropriate locations in the DCD (i.e., DCD Tier 2, Section 2 as well as Table 2.0-1, and DCD Tier 1, Table 5.1-1). Also, provide the technical basis for this definition of the average shear wave velocity and explain how it would compare to the results obtained by properly treating multiple layers of varying shear wave velocities.*

F) *In the same discussion (Item 3 on page 12 of 34 - Evaluation of Results), the statement is made that "this velocity ratio condition does not apply to the FWSC nor to the RB/FB and CB if founded on rock-like material having a shear wave velocity of 1067 m/sec (3500 ft/sec) or higher." The definition of "rock" material, following the guidance of the SRP Section 3.7.2, associated with SSI evaluations is not 3,500 fps but 8,000 fps after which SSI effects are considered small. Provide the numerical results available to indicate that the computation of maximum toe pressure is not impacted by the velocity ratios for cases where the layer beneath the basemat has velocities greater than 3,500 fps.*

G) *In DCD Tier 1, Table 5.1-1 and DCD Tier 2, Table 2.0-1, the descriptions provided for minimum static and minimum dynamic bearing capacity are not clear. These requirements should be specified as "maximum bearing demand" not "minimum bearing capacity" since these values were obtained from the envelope of the elastic SASSI results applied to the liftoff calculations. The COL applicant then needs to determine the allowable bearing pressure based on the site-specific soil "bearing capacity" divided by the factor of safety appropriate for the design load combination. Therefore, the DCD should be revised to capture the following items: (1) present the values as maximum static bearing demand and maximum dynamic bearing demand, and (2) expand the footnote applicable to these values to state that the allowable bearing pressure shall be developed from the site-specific bearing capacity divided by a factor of safety appropriate for the design load combination.*

H) *In Section 3A.8.8, there is no indication that the torsional seismic effects are included in developing the soil pressures for the design of the foundation walls, along with the wall pressures from the translational seismic loadings. Explain how*

the torsional seismic effects have been included in the design of the foundation walls.

I) In several of the enveloping floor response spectra (e.g., Figures 3.8-94(19), (20), and (22), the staff noted that "valleys" exist between successive peaks in the low frequency region, up to approximately 5 Hz. If the spectral peaks are influenced by site conditions, it is the staff's position that these "valleys" should be filled-in to accommodate the expected variability in site shear wave profiles that may be encountered for this generic design. GEH is requested to provide an explanation why these valleys have not been filled-in.

J) In item (3) on page 14 of 34, Table 3.8-94(5) – Maximum Dynamic Soil Bearing Stress Involving SSE + Static, the bearing pressures under soft, medium and hard soils for each of the three structures (RB/FB, CB, and FWSC) are presented. For the CB, the tabulated bearing pressures are 0.44 MPa for soft, 2.2 MPa for medium, and 0.42 MPa for hard soils. These values show a very large variation between the medium soil values and the other two values, unlike the RB/FB and FWSC, where a more gradual variation exists. Therefore, GEH is requested to explain why the bearing pressure for the CB medium soil case varies by a factor of five times from the soft and hard soil cases.

GEH Response

A) A refined bearing pressure time history analysis for all time steps has been performed. The maximum dynamic soil bearing pressures obtained from this analysis are shown in Table 3.8-94(6). The results of all SASSI cases including layered site soil Cases L-2 and L-4 are included in the analysis. DCD Tier 1 Table 5.1-1 and DCD Tier 2 Tables 2.0-1, 3G.1-58 and 3G.2-27 will be revised in Revision 6 to include these maximum dynamic soil bearing pressures. Please refer to GEH's response to NRC RAI 3.8-94 S04, Item D) below.

B) The Energy Balance Method is based on the assumption that the soil strain energy associated with the rocking of the basemat is the same for the linear response ignoring the uplift effect and for the nonlinear response considering the uplift effect. The source of the Energy Balance Method is a technical paper entitled "Simplified Methods for Predicting Seismic Basemat Uplift of Nuclear Power Plant Structures," by W.S. Tseng and D.D. Liou, presented at the 6th International Conference on SMiRT, August 1981. This technical paper is DCD Tier 2 Reference 3G.1-2.

Contact length CL is a calculated quantity from the Energy Balance calculation. Contact length CW is the width of the foundation.

C) The Energy Balance Method takes into account the effects of uplift on the linear response calculated by SASSI.

In the technical paper "Simplified Methods for Predicting Seismic Basemat Uplift of Nuclear Power Plant Structures," by W.S. Tseng and D.D. Liou in GEH's response

to NRC RAI 3.8-94 S04, Item B), the Energy Balance Method was developed on the basis of a comparison of results of both linear and nonlinear time history analyses. It is concluded that the proposed simplified method provides a reasonable estimate using the linear analysis results when the amount of uplift is within 50% of the basemat dimension.

The SASSI results for the RB/FB layered site soil Case RL-2 are examined for the extent of maximum uplift when the bearing pressure reaches maximum in combination with dead loads and buoyancy. As shown in Figure 3.8-94(40), the extent of uplift is not extensive and a large portion of the basemat remains in contact with the soil.

D) Layered site soil Cases L-2 and L-4 are no longer excluded from the foundation stability evaluation, and all layered site soil cases are considered in the ESBWR Standard Plant design. DCD Tier 2 Subsections 3A.8.7 and 3A.9.3 will be revised in Revision 6 to include layered site soil Cases L-2 and L-4. Please refer to GEH's response to NRC RAI 3.8-94 S04, Item A).

E) The new ESBWR Standard Plant site interface parameter for the maximum ratio of soil shear wave velocities in adjacent layers, as proposed in GEH's response to NRC RAIs 3.8-94 S03 (MFN 06-407 S13, dated 2/20/09) and 3.8-96 S03 (MFN 06-407 S14, dated 2/20/09), will not be included in Revision 6 of DCD Tier 2 Table 2.0-1. Please refer to GEH's response to NRC RAI 3.8-94 S04, Item D).

F) Please refer to GEH's response to NRC RAI 3.8-94 S04, Item E).

G) In Revision 6 of DCD Tier 1 Table 5.1-1, DCD Tier 2 Section 2.0 and DCD Tier 2 Table 2.0-1, the descriptions "Minimum Static Bearing Capacity" and "Minimum Dynamic Bearing Capacity" will be changed to "Maximum Static Bearing Demand" and "Maximum Dynamic Bearing Demand", respectively. DCD Tier 1 Table 5.1-1 Note (2) and DCD Tier 2 Table 2.0-1 Note (7) will be expanded to state that the allowable bearing pressure is developed from the site-specific bearing capacity divided by a factor of safety appropriate for the design load combination.

H) Torsional seismic effects have been included in the design of the foundation walls. The SASSI model used is a 3D model including the torsional degree of freedom. Therefore, the calculated soil pressures include the torsional effects. To evaluate the torsional contribution, the SASSI calculated pressures at two ends and at the center of the wall are shown in Figures 3.8-94(41) and 3.8-94(42) for RB/FB layered site soil Case RL-2 and the CB layered site soil Case CL-2, respectively. As shown, the torsional contribution is not significant, since pressures are similar along the wall width. For wall design the SASSI calculated pressures along the wall width at a given elevation are averaged and applied as uniform pressures. Furthermore, as stated in DCD Tier 2 Section 3A.8.8, the wall design pressures are the envelope of the SASSI results and the ASCE 4-98 elastic solution. Although the torsional effect is not addressed in the ASCE 4-98 elastic solution, the inclusion of the ASCE 4-98 results in the design envelope provides additional margins above the SASSI results.

Hence, the foundation walls are adequately designed for torsion-induced seismic soil pressures.

I) Sufficient levels of conservatism are already built into the design floor response spectra in the form of enveloping and peak broadening the results of a sufficient number of generic sites under a bounding Certified Seismic Design Response Spectra (CSDRS) ground input motion. To provide additional margins for sites that might have predominant SSI frequencies at the spectral valleys, the spectral valleys of the site enveloping floor response spectra are further filled-in for the generic design floor response spectra. As an example, the original enveloping floor response spectra at the Vent Wall top, which is the same location as shown in Figure 3.8-94(18), is shown in Figure 3.8-94(43) together with its respective enveloping floor response spectra having the spectral valleys filled-in. The site enveloping floor response spectra in DCD Tier 2 Subsection 3A.9.2 will be replaced in Revision 6 with enveloping floor response spectra having the spectral valleys filled-in. DCD Tier 2 Subsections 3A.8.7 and 3A.9.2 will be revised in Revision 6 for clarification with regards to the spectral valleys being filled-in.

J) According to the SASSI results, the vertical seismic forces for the CB medium site condition are larger than those for the soft and hard site conditions. When a large vertical seismic force is applied upward, the contact length is reduced since the net downward vertical load is decreased. As a result, the bearing pressure at the toe is increased. Table 3.8-94(7) shows the seismic forces when the maximum bearing pressure for the CB occurs. The medium case has a large vertical response. This is the reason why the bearing pressure for the CB medium site condition is larger than other site conditions.

   To gain more insight about the vertical load contribution to bearing pressures for each site condition, Table 3.8-94(8) has been prepared to show the seismic forces at the time when the vertical seismic load is maximum (Vmax). The value of Vmax for the medium site condition is close to that for the hard site. However, Mx and My for the medium site condition are much larger than the hard site condition. Thus, the bearing pressure for the medium site condition becomes larger.

Table 3.8-94(6) Maximum Dynamic Soil Bearing Pressure Involving SSE + Static (MPa)

Building	Site Condition		
	Soft (V_s = 300 m/sec)	Medium (V_s = 800 m/sec)	Hard ($V_s \geq$ 1700 m/sec)
RB/FB	1.1	2.7	1.1
CB	0.50	2.2	0.42
FWSC	0.46	0.69	1.2

Table 3.8-94(7) Seismic Forces at the Time of Maximum Bearing Pressure for CB

	Soft		Medium		Hard	
	Downward	**Upward**	**Downward**	**Upward**	**Downward**	**Upward**
Time (sec)	7.355	7.340	7.155	7.150	6.685	13.60
Mx (MN-m)	302.9	345.6	161.5	160.2	80.5	109.5
My (MN-m)	249.0	157.8	117.3	114.1	147.0	112.8
V (MN)	40	43	91	92	56	10
Total Vertical Load (MPa)	235	51	286	2	251	84
Bearing Pressure (MPa)	0.50	0.28	0.48	2.19	0.42	0.19

Table 3.8-94(8) Seismic Forces at the Time of Maximum Vertical Seismic Load (Vmax) for CB

	Soft		Medium		Hard	
	Downward	**Upward**	**Downward**	**Upward**	**Downward**	**Upward**
Time (sec)	7.150		7.150		7.145	
Mx (MN-m)	85.8		160.2		6.7	
My (MN-m)	69.0		114.1		47.1	
Vmax (MN)	79		92		90	
Total Vertical Load (MPa)	274	15	287	2	285	5
Bearing Pressure (MPa)	0.43	0.07	0.48	2.19	0.41	0.02

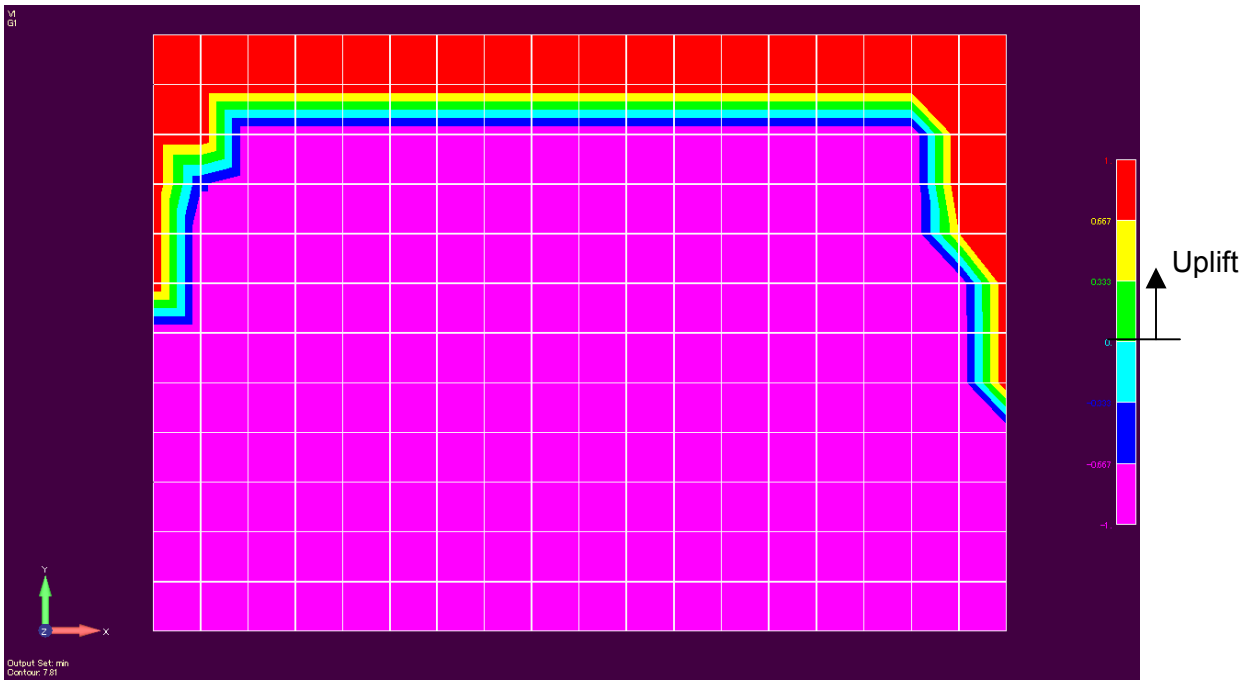

Figure 3.8-94(40) RB/FB Layered Site Soil Case RL-2, Time = 7.810 sec

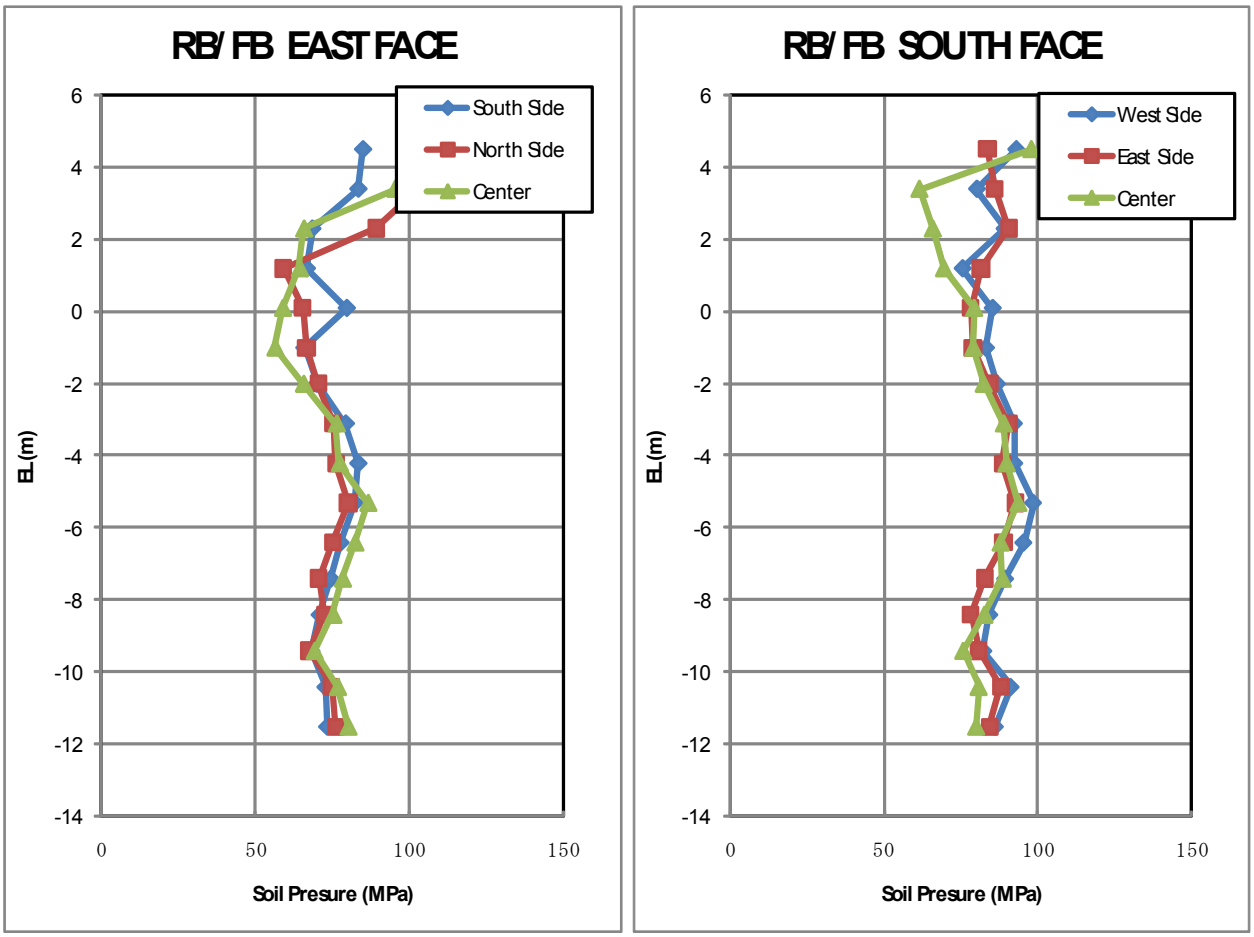

Figure 3.8-94(41) Soil Pressure in SASSI Analysis – RB/FB Layered Site Soil Case RL-2

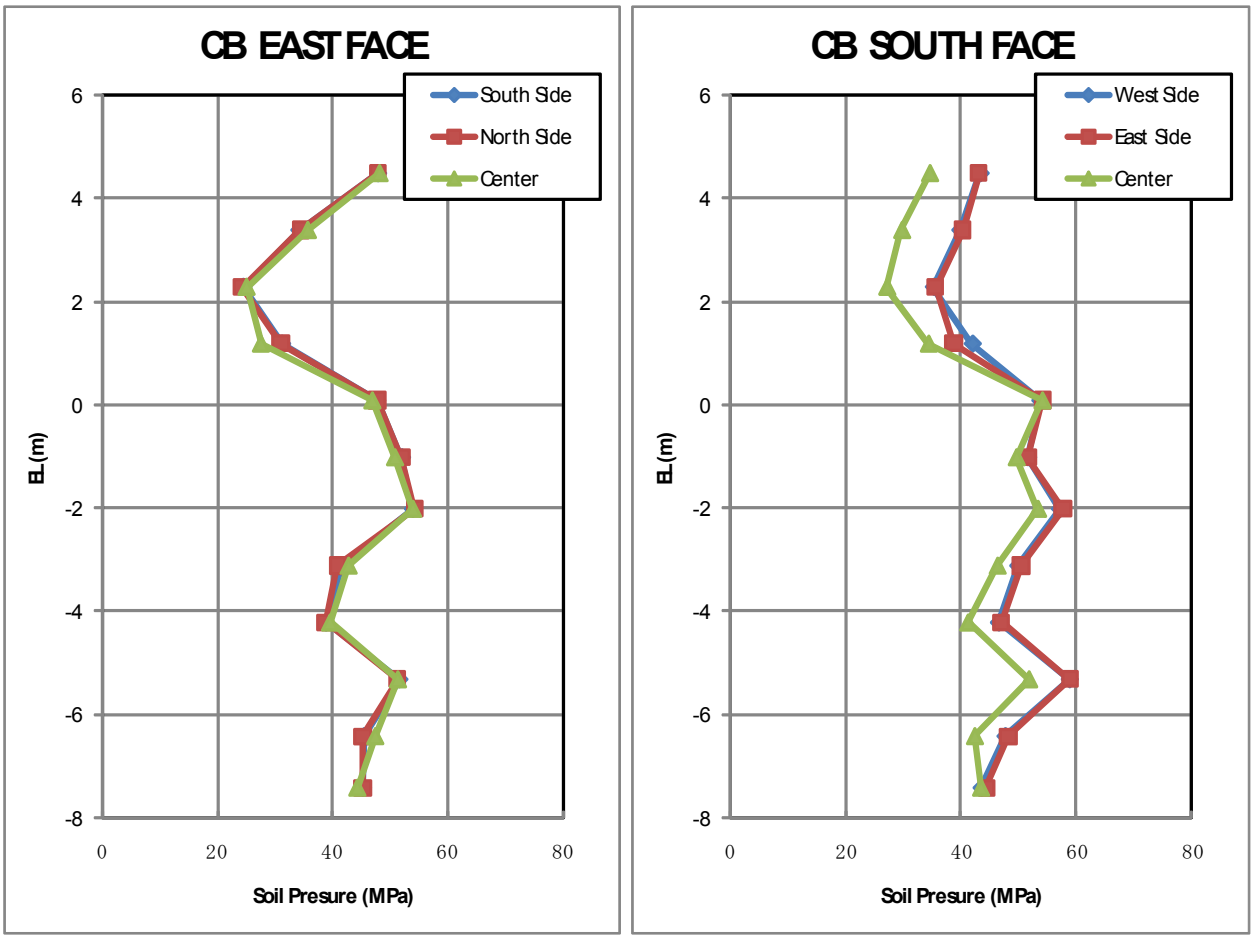

Figure 3.8-94(42) Soil Pressure in SASSI Analysis – CB Layered Site Soil Case CL-2

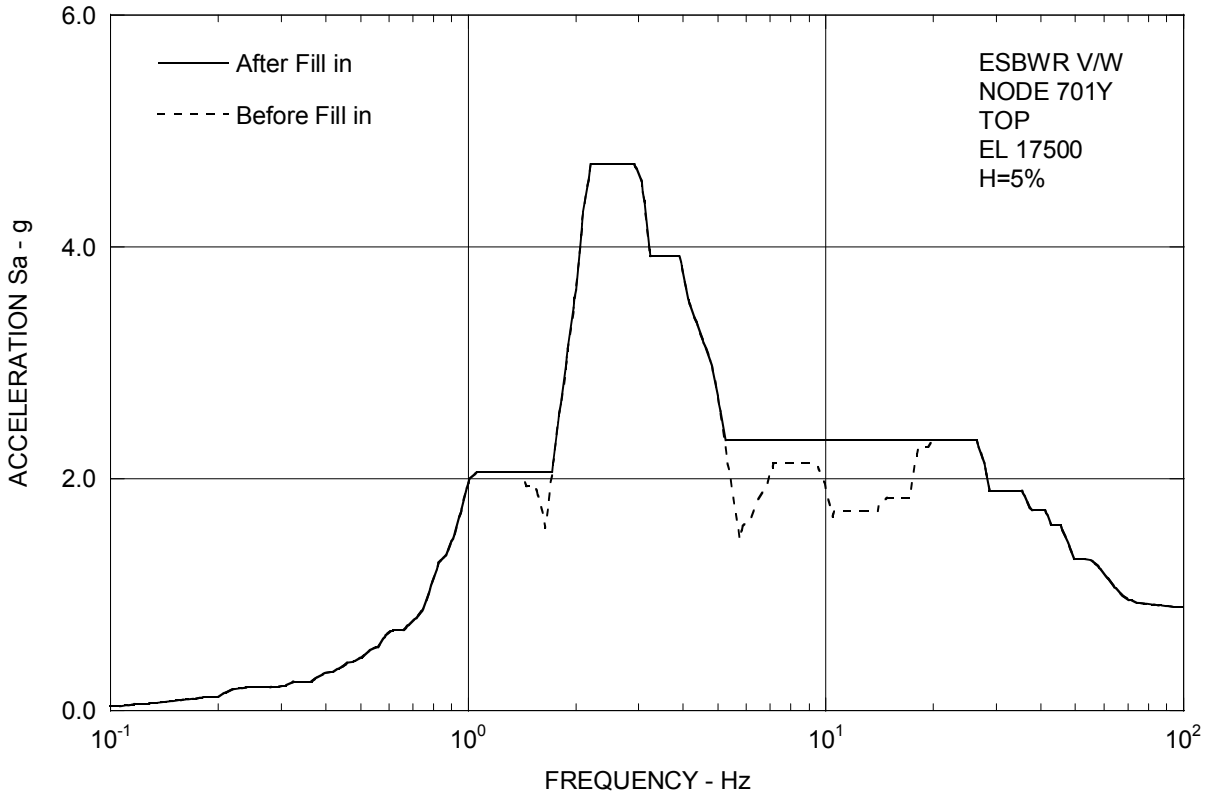

Figure 3.8-94(43) Enveloping Floor Response Spectra – Vent Wall Top Y

DCD Impact

A markup of DCD Tier 1 Table 5.1-1 was provided to the NRC in MFN 09-388, dated 6/12/09.

Markups of DCD Tier 2 Section 2.0, Subsections 3A.8.7, 3A.9.2 and 3A.9.3, Tables 2.0-1, 3G.1-58, 3G.2-27 and 3G.4-23 and Figures 3A.9-1a through 3A.9-1l, 3A.9-2a through 3A.9-2l and 3A.9-3a through 3A.9-3l were provided to the NRC in MFN 09-388, dated 6/12/09.

NRC RAI 3.8-94, Supplement 5

Item B in the RAI 3.8-94 S04 response provided only a one sentence description of the Energy Balance Method (EBM) and identified the source for this method which is a paper presented in the 6th SMiRT conference. A review of this paper has led to the need for GEH to address some items:

1. *The formulation presented in the referenced paper is applicable to circular rigid foundations. Provide justification for use of these formulations for the rectangular foundations for ESBWR. Otherwise, if a new set of formulations were derived for the rectangular foundations at ESBWR, provide the basis for these new formulations.*
2. *In the referenced paper, the results using the EBM were compared with the more accurate nonlinear analysis method that considered uplift appropriately. For most of the responses, it appears that the EBM is unconservative. For example, in the case of the maximum basemat uplift ratio (alpha in percent), the range of underprediction was from 13 percent for the case of 1,000 fps soil shear wave velocity rising to 32 percent for the case of 6,000 fps soil shear wave velocity. Similarly, in the case of maximum basemat moment, the range of underprediction was from 7.5 percent for the case of 3,000 fps soil shear wave velocity rising to 30 percent in the case of 6,000 fps soil shear wave velocity. In view of this substantial underprediction of uplift and basemat moment, what is the basis for still using the EBM to obtain the soil bearing pressure calculation. The paper also discusses a Modified Energy Balance Method (MEB) which appears to be much more accurate when compared to the nonlinear analysis method. Explain why this method wasn't utilized.*
3. *Confirm that the "Contact Width – CW" used in the formulations for bending about the other (perpendicular) horizontal axis corresponds to the full width of the foundation. If this is the case, then explain why the full width is utilized. Has it been determined that no uplift is possible for rotation about the other horizontal axis or that the uplift about both axes do not occur at the same time? The staff notes that if there is uplift possible for rotation about the other horizontal axis, this might cause higher soil bearing pressures than those calculated in the RAI response.*
4. *It appears that the EBM approach calculates not only the uplift, but also a new basemat moment resulting from consideration of the uplift. Therefore, explain whether a new basemat moment was calculated using the EBM approach or the original moment was utilized for calculating the soil bearing pressure. As a sanity check, if a new moment was utilized, then provide the magnitude of the new calculated basemat moment and compare it against the original moment obtained from the envelop of all of the SASSI runs. Also, as a sanity check provide the magnitude of the maximum soil bearing pressure calculated from the envelop of all of the SASSI runs so that a comparison can be made with this new EBM approach.*

Lastly, provide the magnitude of the uplift calculated using the EBM so that a comparison can be made with the extent of implied uplift (i.e., tensile basemat/soil interface loads) shown in Figure 3.8-94(40) of the RAI response. The above requested

information should be provided for all of the structures. The staff notes that based on Table 1 from the referenced paper, if the original moment was used rather than the new moment calculated using the EBM, the basemat moment appears to be conservative in all of the cases studied (when compared to the accurate nonlinear solution) while the new moment appears to underpredict the basemat moment as discussed in item 2 above. Therefore, depending on which moment was used for calculating the soil bearing pressure, one part of item 2 above could be resolved.

GEH Response

(1) The methods presented in the referenced paper identified as DCD Tier 2 Reference 3G.1-2 are the same for both circular and rectangular foundations and the only differences are the parameters related to geometry. The following is the development of the equations for rectangular foundations.

(a) Relationship between Rocking Motion, Overturning Moment and Contact-Area of a Rectangular Foundation

Figure 3.8-94(44) shows the configuration of a rigid rectangular basemat in the uplifted position. The basemat is considered to be supported by a set of uniformly distributed compression (no tension) vertical soil springs having stiffness k_ϕ per unit area, which are determined by the following:

$$k_\phi = K_\phi / I_B \qquad (1)$$

where,

K_ϕ: Rocking spring constant of the rectangular basemat shown in DCD Tier 2 Table 3A.5-1

I_B: Basemat area moment of inertia

$$I_B = \frac{1}{12} C_W D^3$$

Referring to Figure 3.8-94(44), the foundation vertical force *N* and the overturning moment *M* in the uplifted position can be related to soil pressure *p(x)* and the foundation contact length C_L.

$$\begin{aligned} N &= \int_0^{C_L} p(x) C_W \, dx \\ &= k_\phi \phi C_W \int_0^{C_L} (C_L - x) dx \\ &= \frac{1}{2} k_\phi \phi C_W {C_L}^2 \end{aligned} \qquad (2)$$

$$M = \int_0^{C_L} p(x)(D/2 - x)C_W dx$$
$$= k_\phi \phi C_W \int_0^{C_L} (C_L - x)(D/2 - x)dx$$
$$= \frac{1}{12} k_\phi \phi C_W {C_L}^2 [3D - 2C_L]$$
$$= \frac{N}{6}(3D - 2C_L) \quad (3)$$

Rocking rotation and moment at which basemat uplift initiates are the following: ($C_L = D$.)

$$\phi_0 = \frac{2N}{k_\phi C_w D^2} = \frac{ND}{6K_\phi}$$
$$M_0 = \frac{ND}{6} = \frac{\phi_0}{K_\phi} \quad (4)$$

Holding the vertical load as a constant quantity, and varying the contact length *D*, one can determine the relationship between moment *M* and ϕ from equations (2) and (3) for a finite number of variations for C_L.

For the moment *M* larger than the uplift moment M_0, the following relationship can be found by normalizing the *M* and ϕ by the M_0 and ϕ_0.

$$\bar{\phi} = \frac{\phi}{\phi_0} = \frac{2N}{k_\phi C_w {C_L}^2} \Big/ \frac{2N}{k_\phi C_w D^2} = \left(\frac{D}{C_L}\right)^2$$
$$\overline{M} = \frac{M}{M_0} = \frac{N}{6}(3D - 2C_L) \Big/ \frac{ND}{6} = 3 - 2\frac{C_L}{D} = 3 - 2\sqrt{\frac{1}{\bar{\phi}}} \quad (5)$$

(b) Basemat Uplift Prediction and Computation of Soil Pressure

The relationship of the overturning M and rocking rotation is non-linear when $C_L < D$, $M > M_0$ and $\phi > \phi_0$. The Energy Balance Method is based on the consideration that the soil strain energy associated with the rocking of basemat is the same for the linear response ignoring the uplift effect, and for the nonlinear response considering the uplift effect.

The soil strain energy stored in the soil spring in a linear response mentioned above can be expressed as follows:

$$U_e = \frac{1}{2} M_e \phi_e = \frac{1}{2} K_\phi {\phi_e}^2 \quad (6)$$

The soil strain energy in case of uplift can be expressed as follows:

$$U_n = M_n d\phi = \frac{1}{2} M_0 \phi_0 + \int_{\phi_0}^{\phi_n} M_i d\phi_i$$
$$= \frac{1}{2} M_0 \phi_0 + \frac{1}{2} \sum_{i=1}^{n} (M_i + M_{i-1})(\phi_i - \phi_{i-1}) \quad (7)$$

The "Energy Balance Method" stipulates that the above non-linear rocking rotation ϕ_n is determined so that the soil strain energy is equal between U_e in (6) and U_n in (7) as illustrated in Figure 3.8-94(45). Then, the soil pressure is calculated as the maximum stress at the edge as follows:

$$p_{\max} = k_\phi \phi_n C_L \quad (8)$$

According to the referenced paper, the above computation tends to underpredict the uplift. The amount of under prediction tends to be bigger with larger ϕ_n. Therefore, an empirical correction to the "Energy Balance Method" is developed to improve the prediction. The referenced paper introduces a coefficient κ which is the normalized instantaneous secant stiffness of basemat rocking ϕ_n and moment M_n.

$$\kappa = \overline{M} / \overline{\phi} = (M_n / M_0) / (\phi_n / \phi_0) \quad (9)$$

The improved rocking rotation is:

$$\phi_{imp} = \phi_n / \kappa \quad (10)$$

Because κ is less than 1 for $C_L < D$, the upper bound soil maximum stress can be calculated as follows:

$$p_{imp} = p_{\max} / \kappa \quad (11)$$

(2) The above method for improving the rocking rotation and soil pressure is called the "Modified Energy Balance Method (MEB)" in the referenced paper and has been utilized in the ESBWR soil bearing pressure calculations.

(3) To account for potential uplift due to rotation about the other horizontal axis, two separate cases, a) *Mx* using MEB together with *My* with full width C_W and b) *My* using MEB together with *Mx* with full width C_W, were considered as illustrated Figure 3.8-94(46). The final soil bearing pressure is the envelope results of the two cases.

(4) As explained in the item (1), the basemat uplift rotation, moment and the soil pressures are calculated in accordance with the MEB method using the elastic SASSI analysis results as input. Tables 3.8-94(9) through 3.8-94(11) show these values calculated from the MEB for the critical bearing pressures cases of all the structures. The SASSI soil pressure distributions are shown in Figures 3.8-94(47) through 3.8-94(50). It can be concluded that the SASSI pressures are smaller and hence the MEB pressures are conservative.

Table 3.8-94(9) Comparison of Basemat Response and Soil Pressure for RB/FB

Building width X		70 m (NS)					
Building width Y		49 m (EW)					
Total Building Weight		2360 MN					
Buoyancy		652 MN					
Soil Condition		Soft		Medium		Hard	
Critical Analysis Case		RU-8 (Soft)		RL-4		RU-8 (Hard)	
Vertical Seismic Load Direction		downward		upward		downward	
SASSI*	Time (sec)	7.435		7.295		10.650	
	Vertical seismic load (MN)	286		848		468	
	Total vertical load N (MN)	2646		860		2828	
	NS-dir moment Mx(MN-m)	5509		6105		2742	
	EW-dir moment My (MN-m)	5543		25480		6100	
	Soil pressure distribution	No tension		Figure 3.8-94(47)		No tension	
Simplified Method **		EB	MEB	EB	MEB	EB	MEB
NS dir. ↓ EW dir.	Maximum basemat uplift ratio	0.0	0.0	0.0	0.0	0.0	0.0
	Maximum basemat rotation ϕ (10^{-4} rad)	2.71	2.71	0.15	0.15	0.12	0.12
	Maximum basemat moment Mx (MN-m)	5509	5509	6105	6105	2742	2742
	Maximum soil pressure 1 Px (MPa)	0.91	0.91	0.40	0.40	0.89	0.89
	Maximum soil pressure 2 Py (MPa)	---	0.20	---	0.91	---	0.22
	Maximum soil pressure Pxy=Px+Py (MPa)	---	1.1	---	1.3	---	1.1
EW dir. ↓ NS dir.	Maximum basemat uplift ratio	0.0	0.0	59.3	75.5	0.0	0.0
	Maximum basemat rotation ϕ (10^{-4} rad)	3.40	3.40	1.52	4.19	0.14	0.14
	Maximum basemat moment My (MN-m)	5543	5543	15345	21066	6100	6100
	Maximum soil pressure 1 Py (MPa)	0.97	0.97	1.23	2.04	1.04	1.04
	Maximum soil pressure 2 Px (MPa)	---	0.14	---	0.62	---	0.07
	Maximum soil pressure Pyx=Py+Px (MPa)	---	1.1	---	2.7	---	1.1
Envelope of Pxy and Pyx (MPa)		---	1.1	---	2.7	---	1.1

Note *: SASSI analysis is a linear time history analysis with the 3D excitation.

**: EB and MEB stand for energy balance and modified energy balance methods, respectively.

Table 3.8-94(10) Comparison of Basemat Response and Soil Pressure for CB

Building width X		30.3 m (NS)					
Building width Y		23.8 m (EW)					
Total Building Weight		195 MN					
Buoyancy		101 MN					
Soil Condition		Soft		Medium		Hard	
Critical Analysis Case		CL-1		CU-4 (Medium)		CU-4 (Hard)	
Vertical Seismic Load Direction		downward		upward		downward	
SASSI*	Time (sec)	7.355		7.150		6.685	
	Vertical seismic load (MN)	40		92		56	
	Total vertical load N (MN)	235		2		251	
	NS-dir moment Mx(MN-m)	249		160		80	
	EW-dir moment My (MN-m)	303		114		147	
	Soil pressure distribution	No tension		Figure 3.8-94(48)		No tension	
Simplified Method **		EB	MEB	EB	MEB	EB	MEB
NS dir. ↓ EW dir.	Maximum basemat uplift ratio	0.0	0.0	88.8	97.9	0.0	0.0
	Maximum basemat rotation ϕ (10^{-4} rad)	0.90	0.90	0.11	3.14	0.12	0.12
	Maximum basemat moment Mx (MN-m)	249	249	30	32	80	80
	Maximum soil pressure 1 Px (MPa)	0.39	0.39	0.05	0.28	0.37	0.37
	Maximum soil pressure 2 Py (MPa)	---	0.11	---	1.90	---	0.05
	Maximum soil pressure Pxy=Px+Py (MPa)	---	0.50	---	2.2	---	0.42
EW dir. ↓ NS dir.	Maximum basemat uplift ratio	0.0	0.0	87.7	97.5	0.0	0.0
	Maximum basemat rotation ϕ (10^{-4} rad)	1.06	1.06	0.09	2.03	0.06	0.06
	Maximum basemat moment My (MN-m)	303	303	23	25	147	147
	Maximum soil pressure 1 Py (MPa)	0.43	0.43	0.05	0.24	0.40	0.40
	Maximum soil pressure 2 Px (MPa)	---	0.07	---	1.75	---	0.02
	Maximum soil pressure Pyx=Py+Px (MPa)	---	0.50	---	2.0	---	0.42
Envelope of Pxy and Pyx (MPa)		---	0.50	---	2.2	---	0.42

Note *: SASSI analysis is a linear time history analysis with the 3D excitation.

**: EB and MEB stand for energy balance and modified energy balance methods, respectively.

Table 3.8-94(11) Comparison of Basemat Response and Soil Pressure for FWSC

Building width X		52 m (NS)					
Building width Y		20 m (EW)					
Total Building Weight		169 MN					
Buoyancy		18 MN					
Soil Condition		Soft		Medium		Hard	
Critical Analysis Case		FL-1		FL-2		FU-2 (Hard)	
Vertical Seismic Load Direction		downward		upward		upward	
SASSI*	Time (sec)	7.145		7.145		6.290	
	Vertical seismic load (MN)	89		104		119	
	Total vertical load N (MN)	258		47		32	
	NS-dir moment Mx(MN-m)	586		587		1332	
	EW-dir moment My (MN-m)	495		602		413	
	Soil pressure distribution	No tension		Figure 3.8-94(49)		Figure 3.8-94(50)	
Simplified Method **		EB	MEB	EB	MEB	EB	MEB
NS dir. ↓ EW dir.	Maximum basemat uplift ratio	0.0	0.0	18.4	22.2	68.1	84.4
	Maximum basemat rotation ϕ (10^{-4} rad)	0.89	0.89	0.04	0.05	0.04	0.18
	Maximum basemat moment Mx (MN-m)	586	586	560	590	653	829
	Maximum soil pressure 1 Px (MPa)	0.31	0.31	0.11	0.12	0.19	0.39
	Maximum soil pressure 2 Py (MPa)	---	0.14	---	0.22	---	0.76
	Maximum soil pressure Pxy=Px+Py (MPa)	---	0.46	---	0.34	---	1.2
EW dir. ↓ NS dir.	Maximum basemat uplift ratio	0.0	0.0	61.1	77.4	61.5	77.9
	Maximum basemat rotation ϕ (10^{-4} rad)	1.63	1.63	3.12	9.26	0.09	0.27
	Maximum basemat moment My (MN-m)	495	495	349	472	237	319
	Maximum soil pressure 1 Py (MPa)	0.39	0.39	0.23	0.40	0.16	0.28
	Maximum soil pressure 2 Px (MPa)	---	0.07	---	0.29	---	0.67
	Maximum soil pressure Pyx=Py+Px (MPa)	---	0.46	---	0.69	---	1.0
Envelope of Pxy and Pyx (MPa)		---	0.46	---	0.69	---	1.2

Note *: SASSI analysis is a linear time history analysis with the 3D excitation.

**: EB and MEB stand for energy balance and modified energy balance methods, respectively.

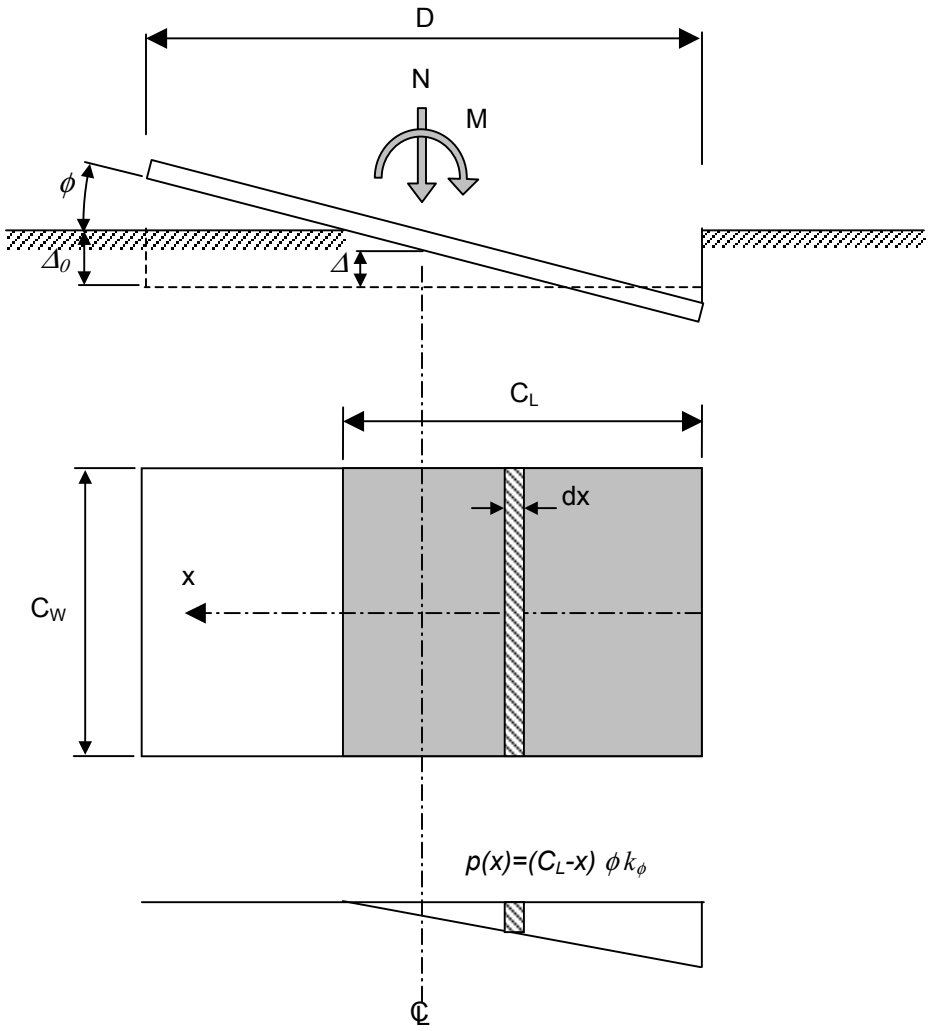

Figure 3.8-94(44) Basemat Configuration and Pressure Distribution

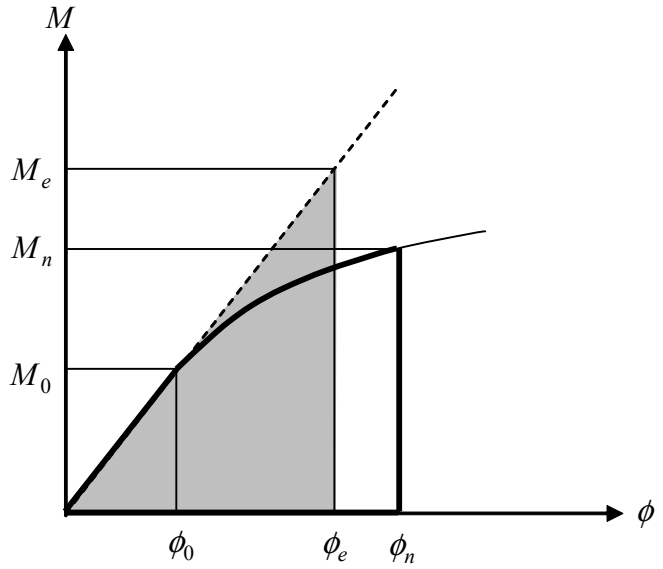

Figure 3.8-94(45) Modified Energy Balance Method

Procedures:

(1) Obtain uplift rotation ϕ_n from the following condition.

Area 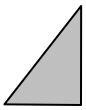 = Area 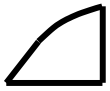 .

(2) Calculated improvement factor κ as follows.

$$\kappa = (M_n / M_0) / (\phi_n / \phi_0)$$

(3) Obtain the improved rotation ϕ_{imp} as follows.

$$\phi_{imp} = \phi_n / \kappa$$

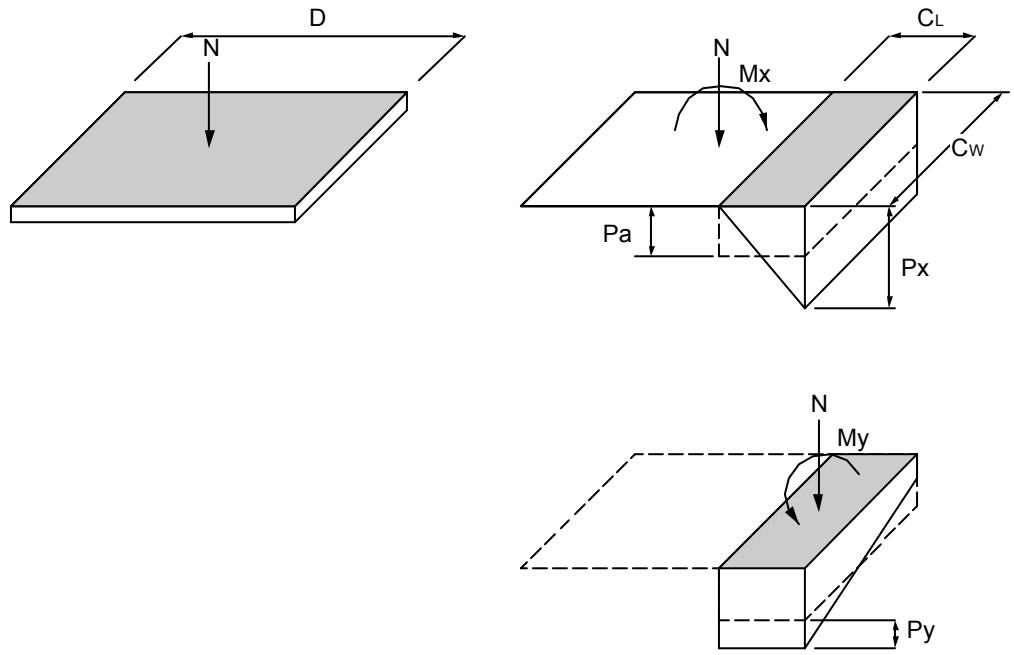

Figure 3.8-94(46) Soil Pressures due to Moments in Two Directions

Procedures:

(1) Maximum soil pressure due to one vertical load and two horizontal moments is calculated by the following equation.

$$P_{xy} = Px + Py$$

where,

Px: Soil pressure obtained by Modified Energy Balance Method considering *N* and *Mx*.

Py: Additional soil pressure due to *My* in the perpendicular direction.

$$Py = My / Z = 6My / (C_L C_W{}^2)$$

(2) The calculation is repeated for the other horizontal direction.

$$P_{yx} = Py + Px$$

where,

Py: Soil pressure obtained by Modified Energy Balance Method considering *N* and *My*.

Px: Additional soil pressure due to *Mx* in the perpendicular direction.

$$Px = Mx / Z = 6Mx / (C_L C_W{}^2)$$

(3) The larger value of P_{xy} and P_{yx} is taken for the maximum soil pressure.

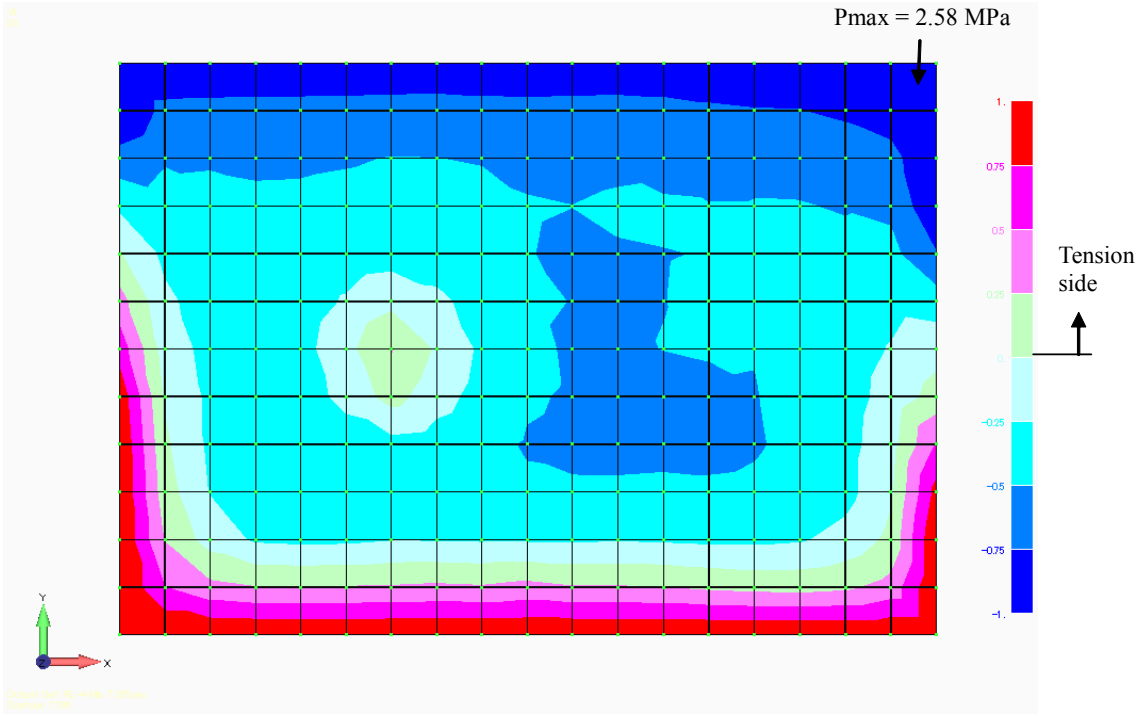

Figure 3.8-94(47) Soil Pressures of SASSI for RB/FB at Medium Site Case RL-4, Time = 7.295 sec

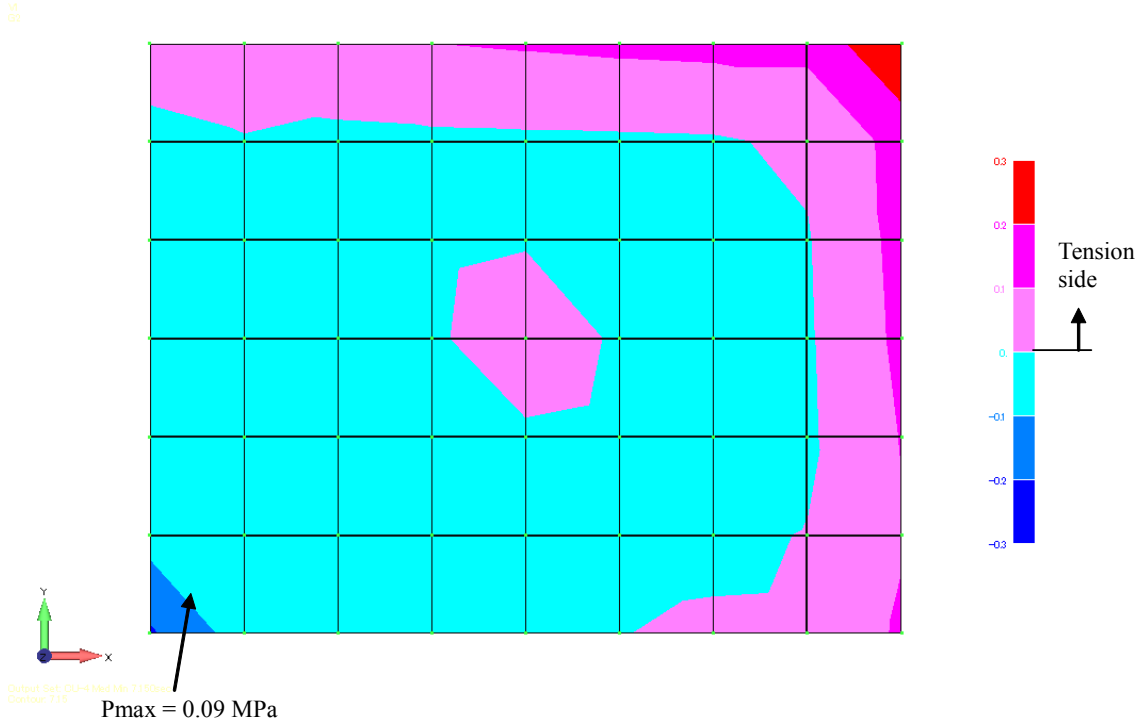

Figure 3.8-94(48) Soil Pressures of SASSI for CB at Medium Site Case CU-4 (Medium), Time = 7.150 sec

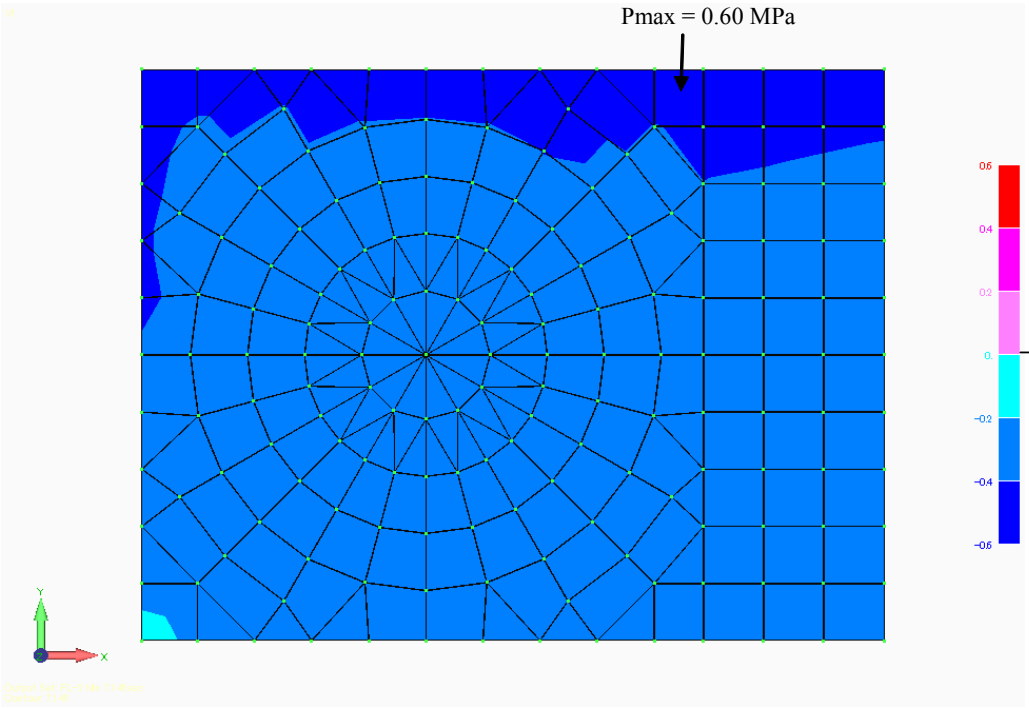

Figure 3.8-94(49) Soil Pressures of SASSI for FWSC at Medium Site Case FL-2, Time = 7.145 sec

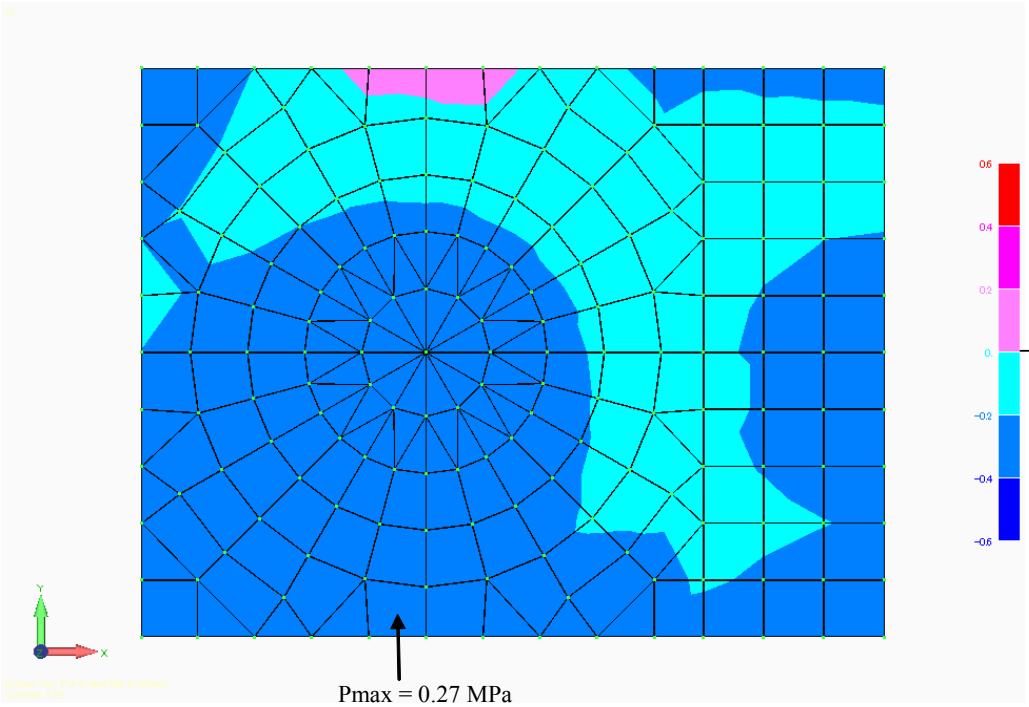

Figure 3.8-94(50) Soil Pressures of SASSI for FWSC at Hard Site Case FU-2 (Hard), Time = 6.290 sec

DCD Impact

No DCD change is required in response to this RAI Supplement.